Towards scale-resolving simulations of industrial relevant turbulent flows

O. Lehmkuhl

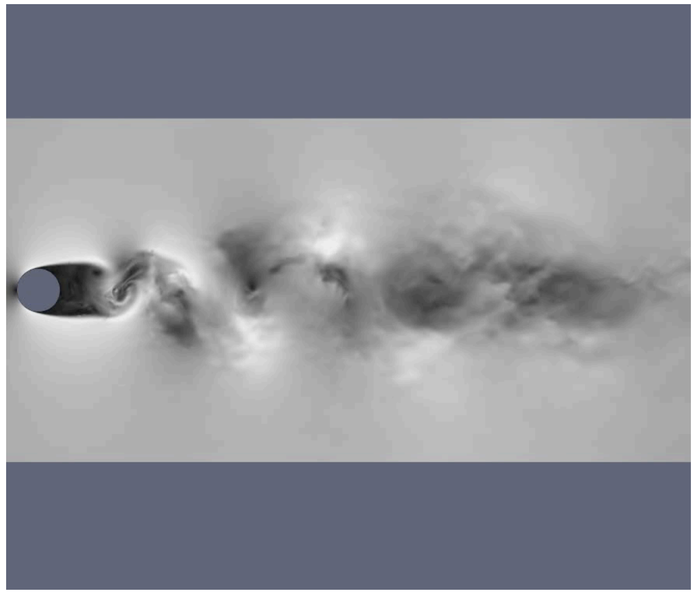


Dpt. Computer Applications in Science and Engineering
Barcelona Supercomputing Center (BSC), Barcelona, Spain

Advanced Modeling & Simulation (AMS) Seminar Series
NASA Ames Research Center, May 13th, 2021

Motivation

Evolution of LES of bluff bodies from 2005 to present (in my world!)

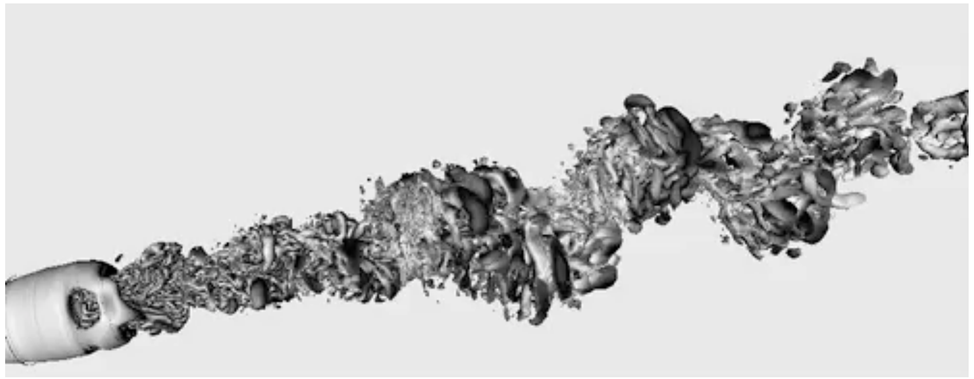


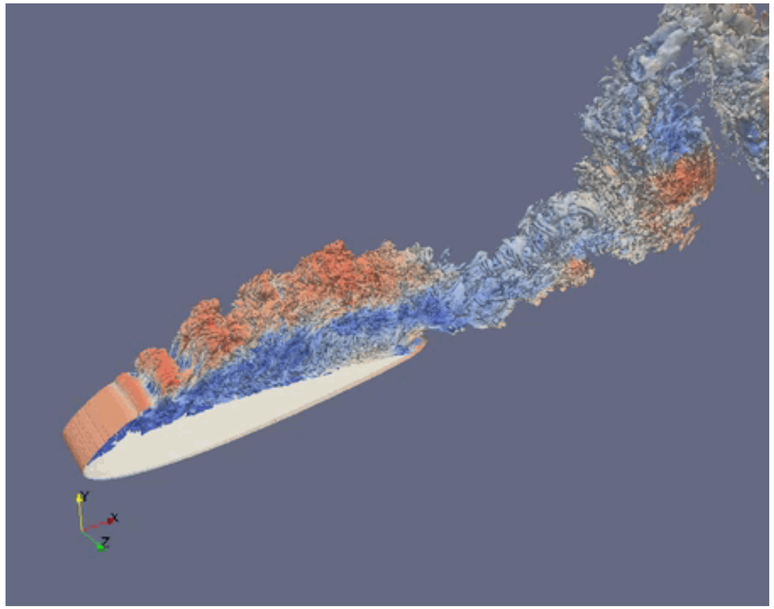


JFF-UPC cluster



Marenostrum 2





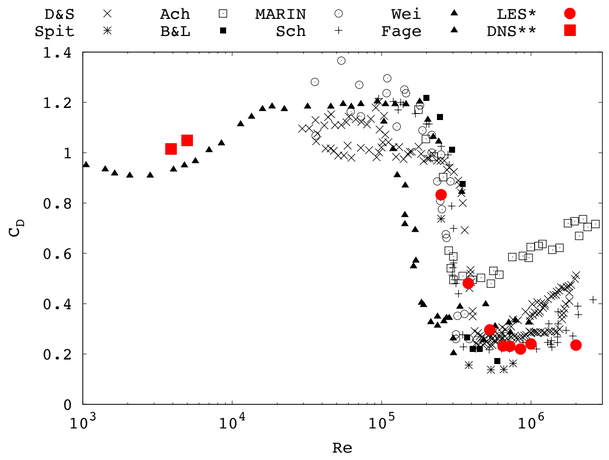
Barcelona Supercomputer

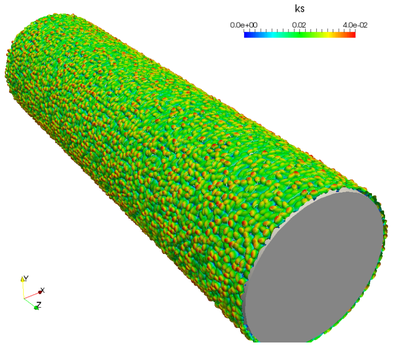
Motivation

Evolution of LES of bluff bodies from 2005 to present (in my world!)



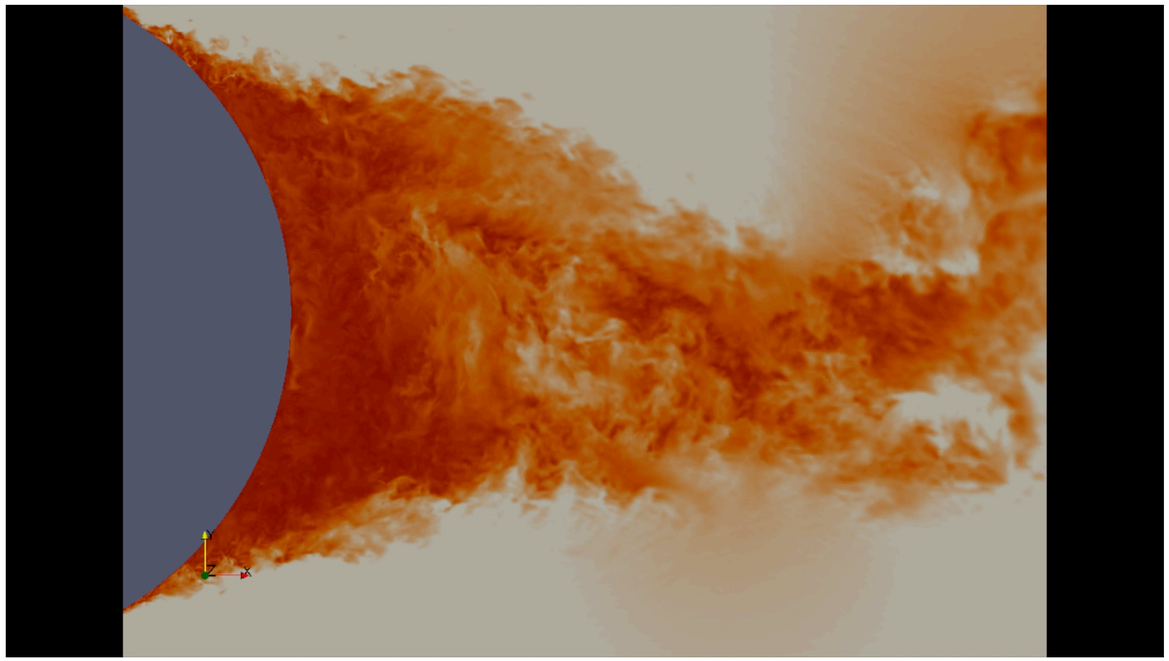
Marenostrum 3



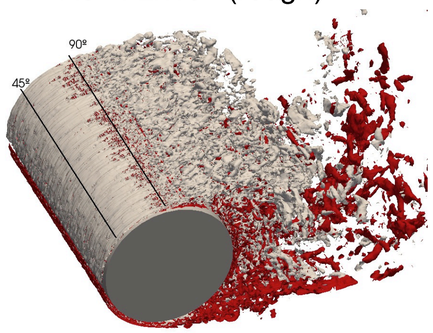




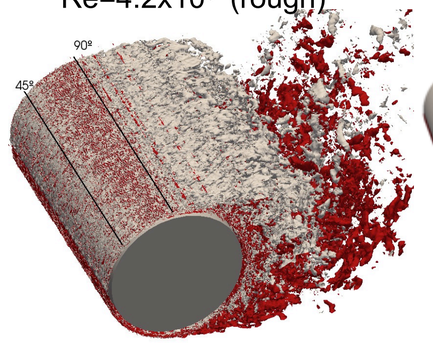
Marconi



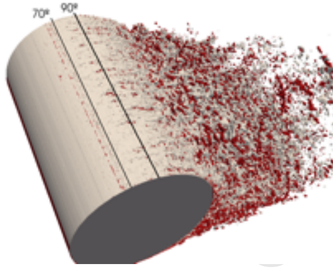
Re=4.2x10^4 (rough)



Re=4.2x10^5 (rough)



Re=5.3x10^5 (smooth



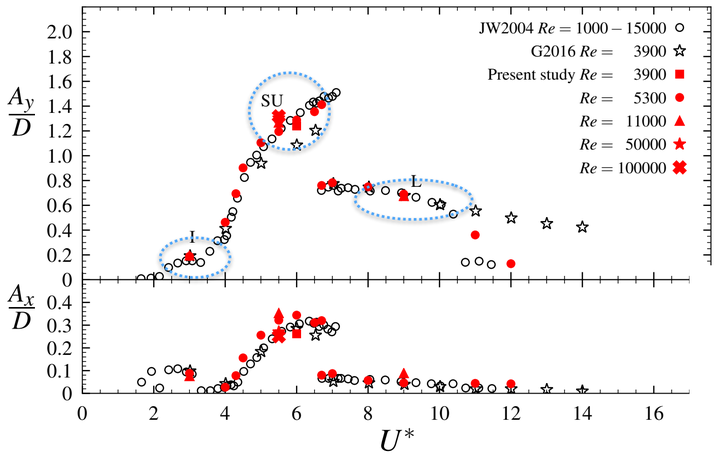
Barc

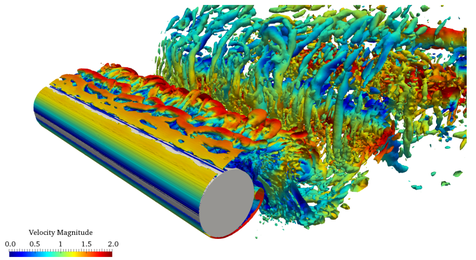
Motivation

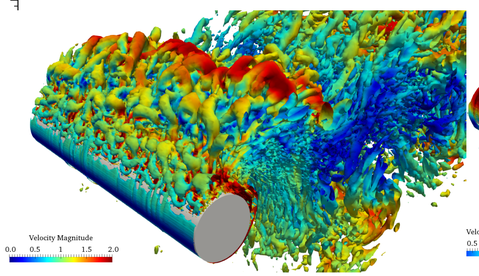
Evolution of LES of bluff bodies from 2005 to present (in my world!)

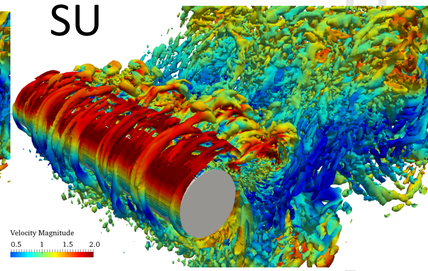


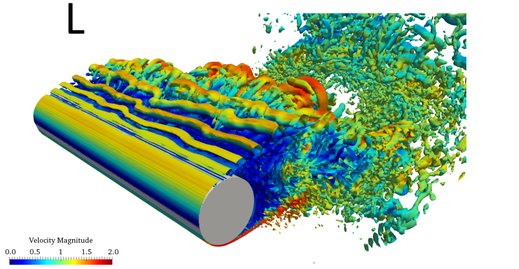
Marenostrum 4 / Super Muc

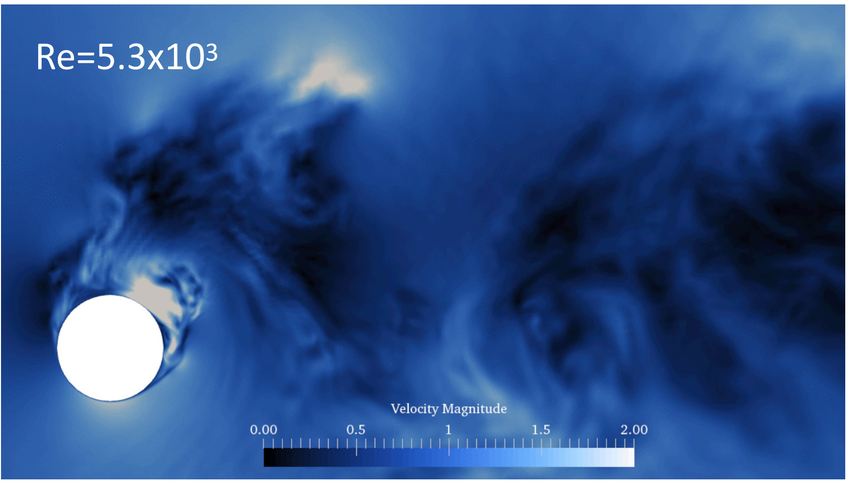


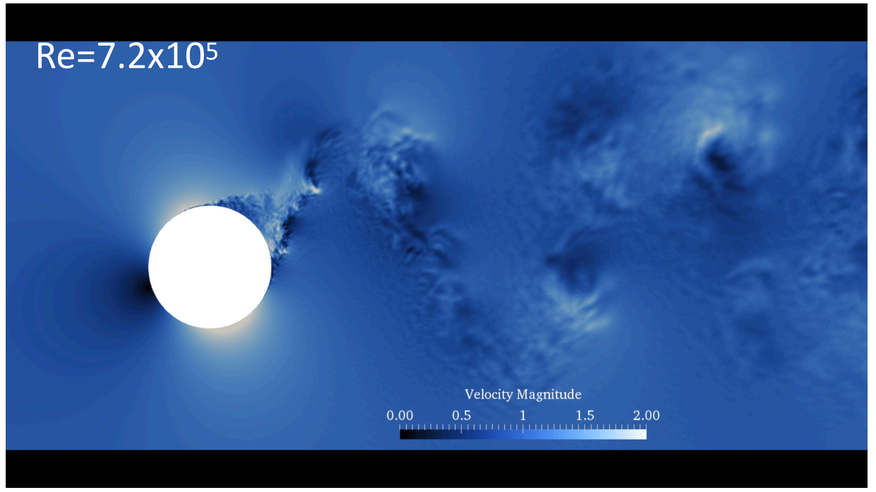












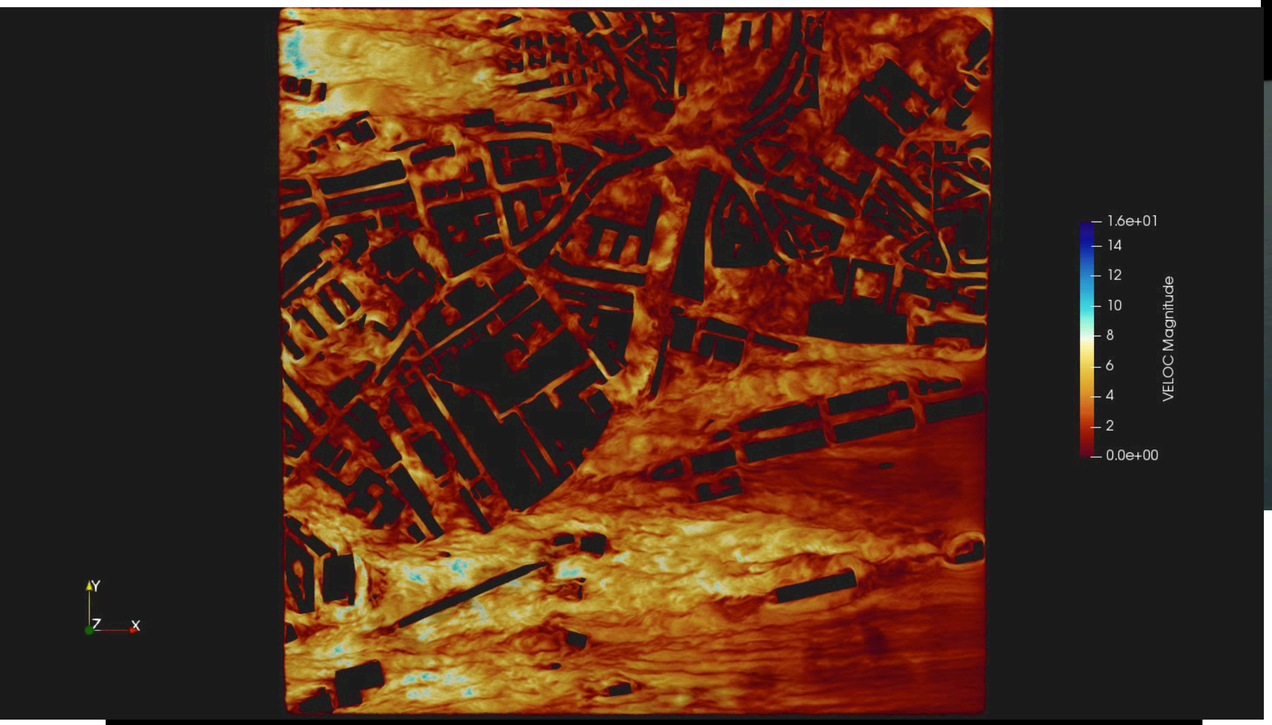
Barcelona Supercomputing Center

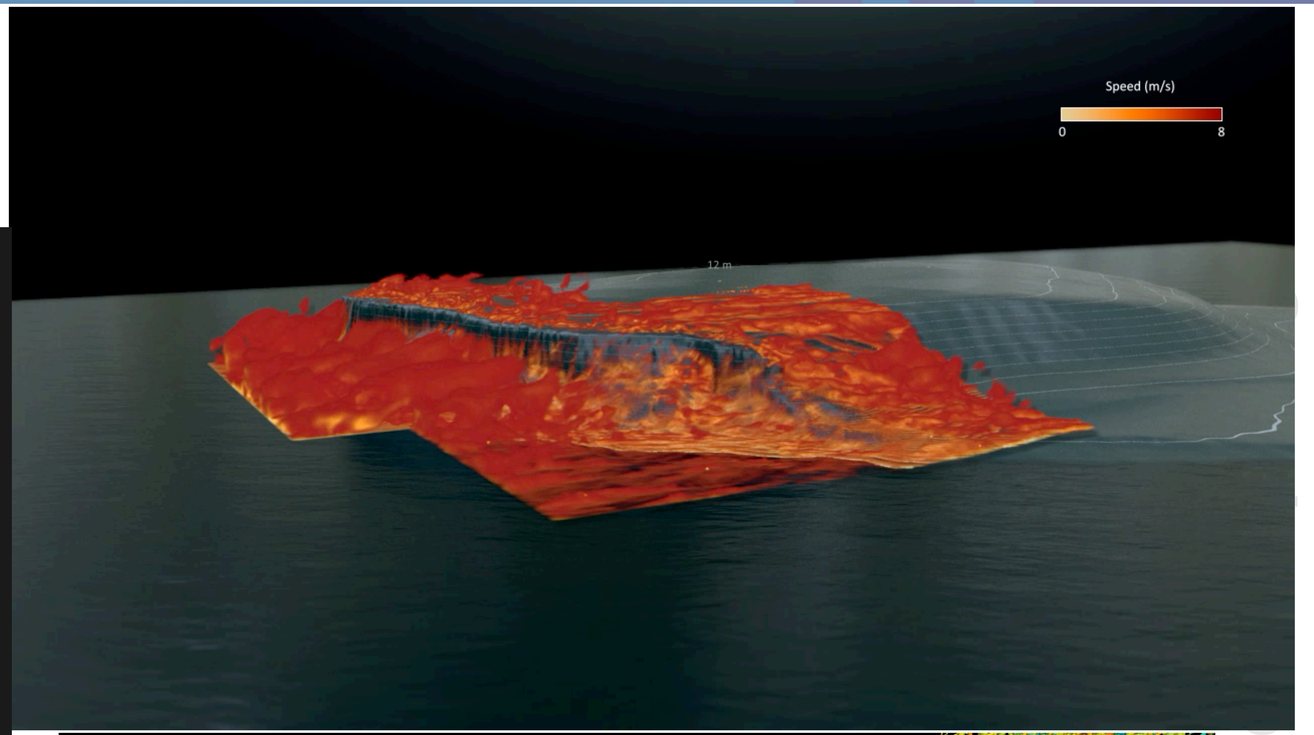
Motivation: what is next?

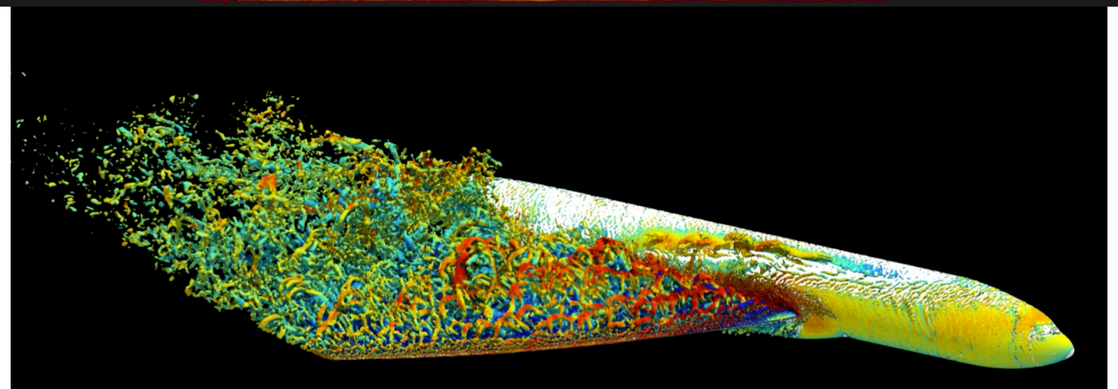
Turbulent flows still need modelling

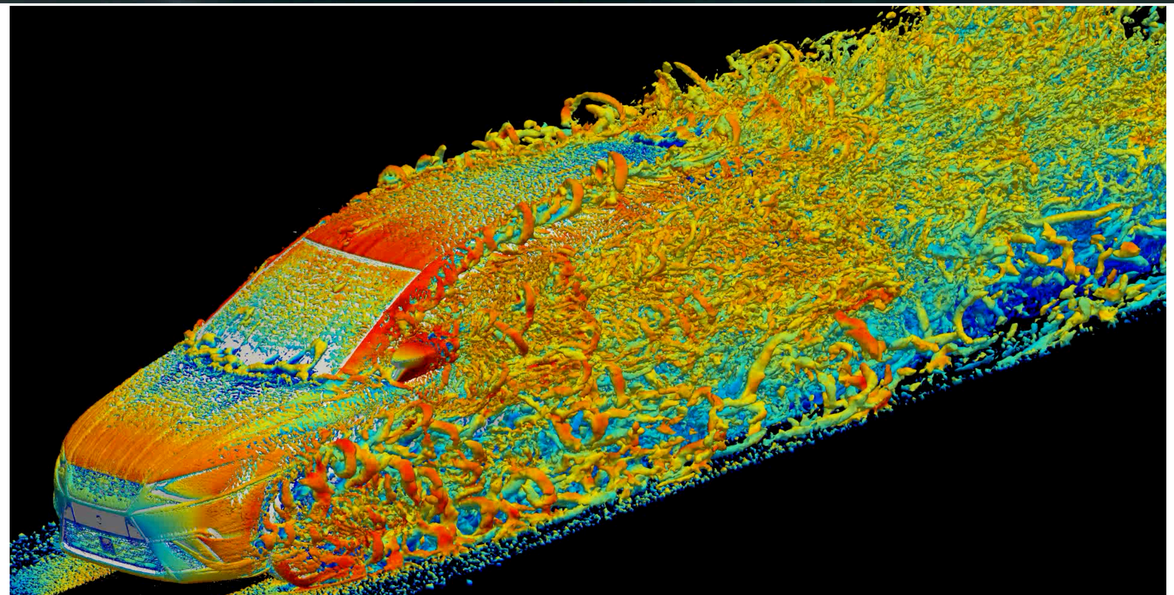
wrLES, O(1B) elements, O(10^8) time steps

wmLES, O(100M) elements, O(10^6) time steps







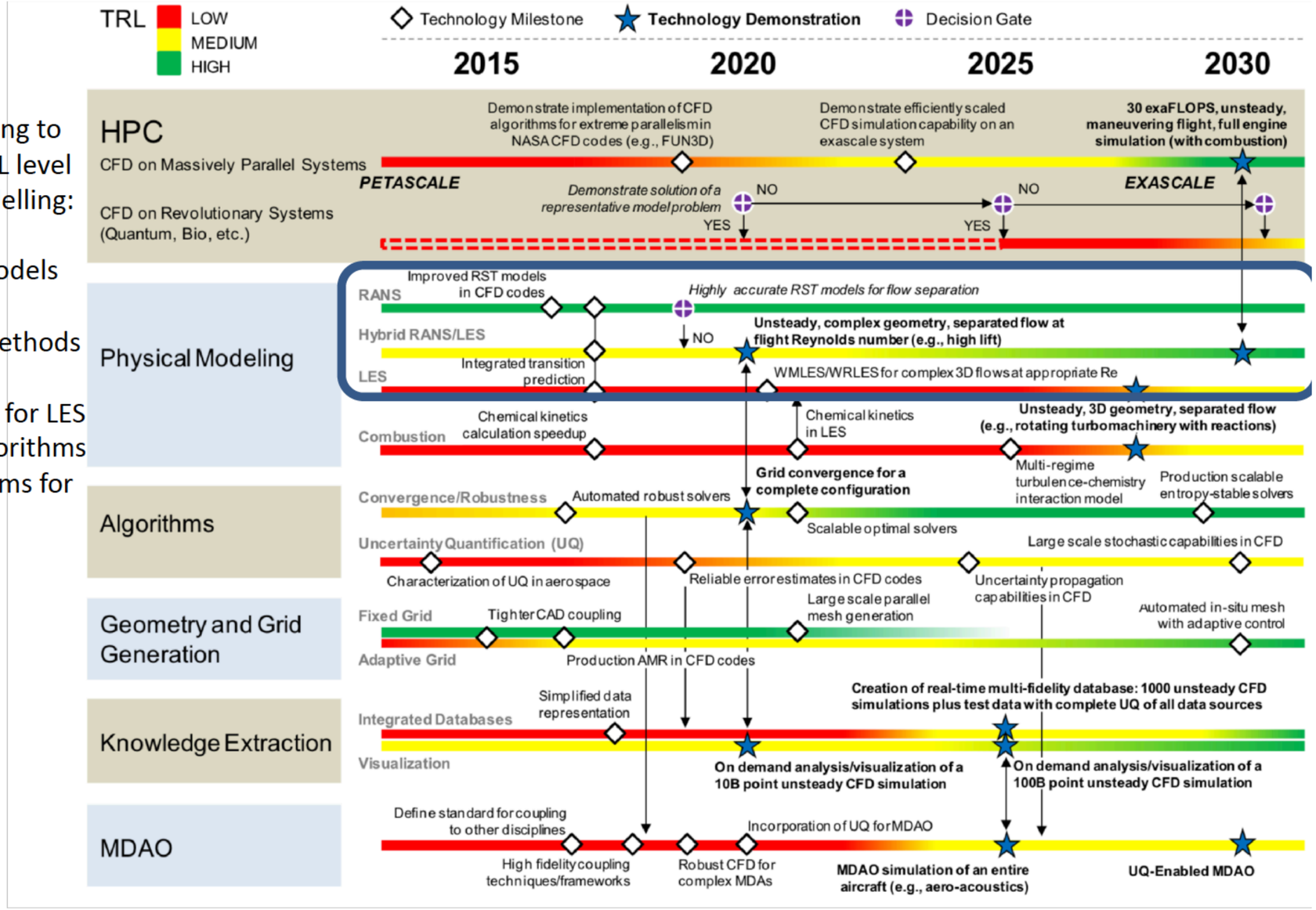


Barcelona Sup

Motivation: what is next?

BSC is researching to increase the TRL level for the LES modelling:

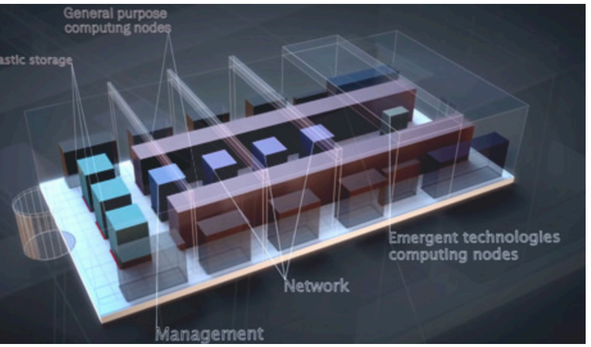
- Novel LES models
- Innovative numerical methods for LES
- Wall-models for LES
- Meshing algorithms
- HPC algorithms for CFD



* ***CFD Vision 2030 Study: A Path to Revolutionary Computational Aerosciences*** , NASA/CR–2014-218178

Barcelona Supercomputing Center

Alya software for large scale CFD



- We use the same methodology for industrial and basic research
- All the levels of simulation are improved by our software development cycle (we do Tier 0 HPC projects and SME projects without distinction)
- HPC a must to enable our high fidelity vision: exascale may be an enabler

+

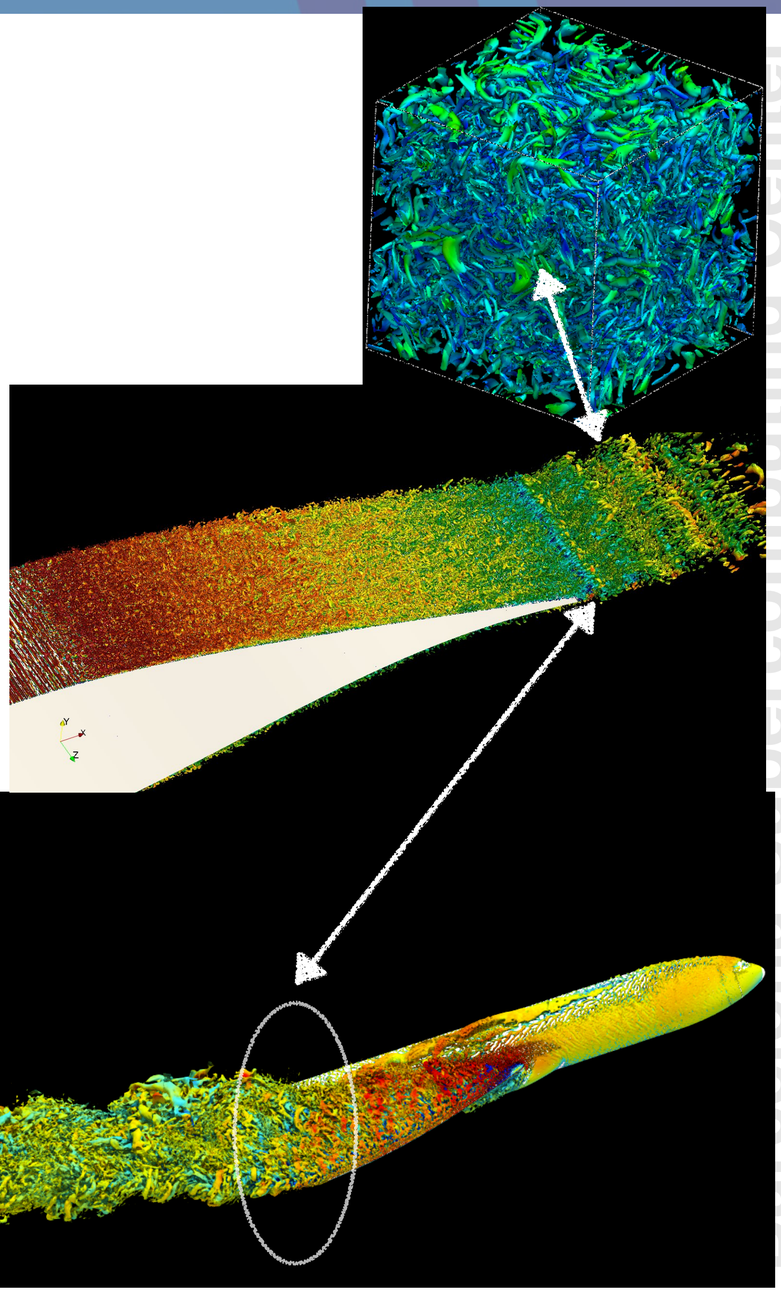
$$\frac{\partial \mathbf{u}}{\partial t} + C(\mathbf{u}) + \nabla p - \nu \Delta \mathbf{u} = \mathbf{f}$$

$$\mathrm{div}\mathbf{u} = 0$$

+

```
do igaus = 1,pgaus

   fact0(DEF_VECT) = gpden(DEF_VECT,igaus) * gpvol(DEF_VECT,igaus)
   fact2(DEF_VECT) = 0.0_rp
   do idime = 1,ndime
      fact2(DEF_VECT) = fact2(DEF_VECT) + gpgve(DEF_VECT,idime,idime,igaus)
   end do
   fact2(DEF_VECT) = fact2(DEF_VECT) * fact0(DEF_VECT)
   !
   ! rho * (div u) u
   !
   do inode = 1,pnode
      do jnode = 1,pnode
         do idime = 1,ndime
            idofv = (inode-1)*ndime+idime
            jdofv = (jnode-1)*ndime+idime
            elauu(DEF_VECT,idofv,jdofv) = elauu(DEF_VECT,idofv,jdofv) &
                 + fact2(DEF_VECT) * gpsha(DEF_VECT,inode,igaus) * gpsha(DEF_VECT,jnode,igaus)
         end do
      end do
   end do
   !
   ! rho * u.grad(u)^t
   !
   do inode = 1,pnode
      do idime = 1,ndime
         idofv = (inode-1)*ndime+idime
         do jnode = 1,pnode
            do jdime = 1,ndime
               jdofv = (jnode-1)*ndime+jdime
               elauu(DEF_VECT,idofv,jdofv) = elauu(DEF_VECT,idofv,jdofv) &
                    + fact0(DEF_VECT) * gpsha(DEF_VECT,inode,igaus) * gpcar(DEF_VECT,idime,jnode,igaus)
            end do
         end do
```



Large eddy simulation models: challenges and bottlenecks

By spatially filtering the NS equations:

$$\frac{\partial \overline{u}_i}{\partial x_i} = 0$$

$$\frac{\partial \overline{u}_i}{\partial t} + \frac{\partial \overline{u}_i \overline{u}_j}{\partial x_j} - \nu \frac{\partial^2 \overline{u}_i}{\partial x_j \partial x_j} + \rho^{-1} \frac{\partial \overline{p}}{\partial x_i} - F_i = -\frac{\partial \mathcal{T}_{ij}}{\partial x_j}$$

$$\mathcal{T}_{ij} - \frac{1}{3}\mathcal{T}_{kk}\delta_{ij} = -2\nu_{sgs}\overline{\mathcal{S}}_{ij}$$

- Smagorinsky
- Dynamic Smagorinsky
- Wall-Adapting Local Eddy-Viscosity (WALE) Model
- **Vreman:**

$$\nu_t = c\sqrt{\frac{B_\beta}{\alpha_{ij}\alpha_{ij}}}$$

$$c = 0.1$$

$$\alpha_{ij} = \boldsymbol{S} = S_{ij}$$

$$\beta_{ij} = \Delta_m^2 \alpha_{mi}\alpha_{mj}$$

$$B_\beta = \beta_{11}\beta_{22} - \beta_{12}^2 + \beta_{11}\beta_{33} - \beta_{13}^2 + \beta_{22}\beta_{33} - \beta_{23}^2$$

Specific challenges:

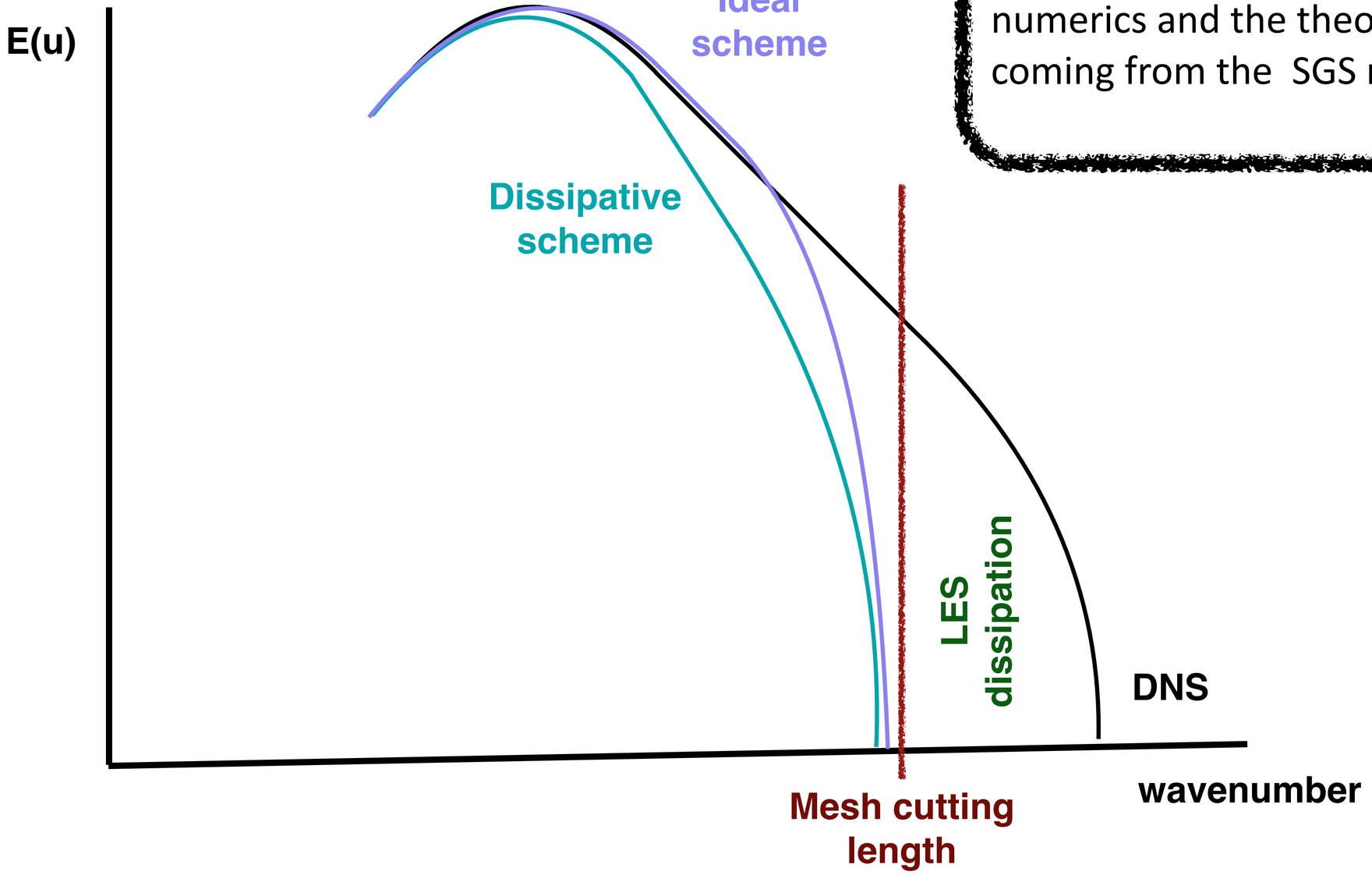
- **Numerics interact with the LES model**
- **Usually the mesh is the filter**
- **Scales at the wall are case dependent**
- **More sensible to geometry and boundaries**

Barcelona Supercomputing Center

Numerics can interact with the SGS model

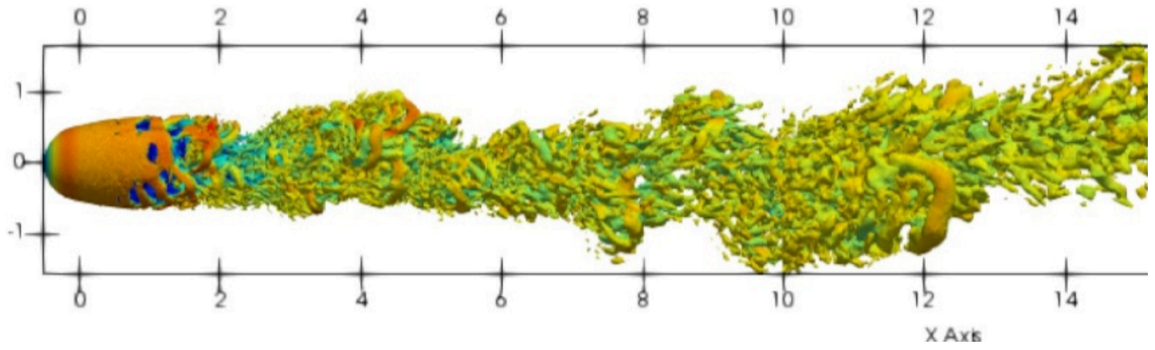
Why this matter?

There is a constant inter-play between numerics and the theoretical dissipation coming from the SGS model

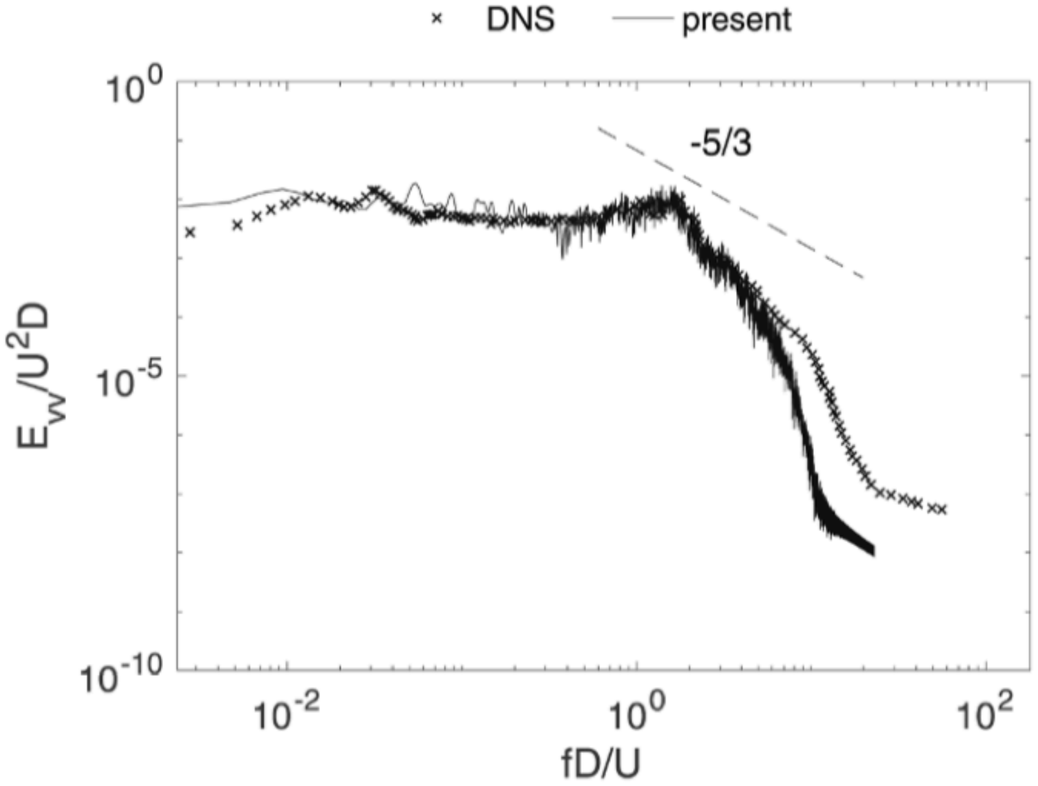


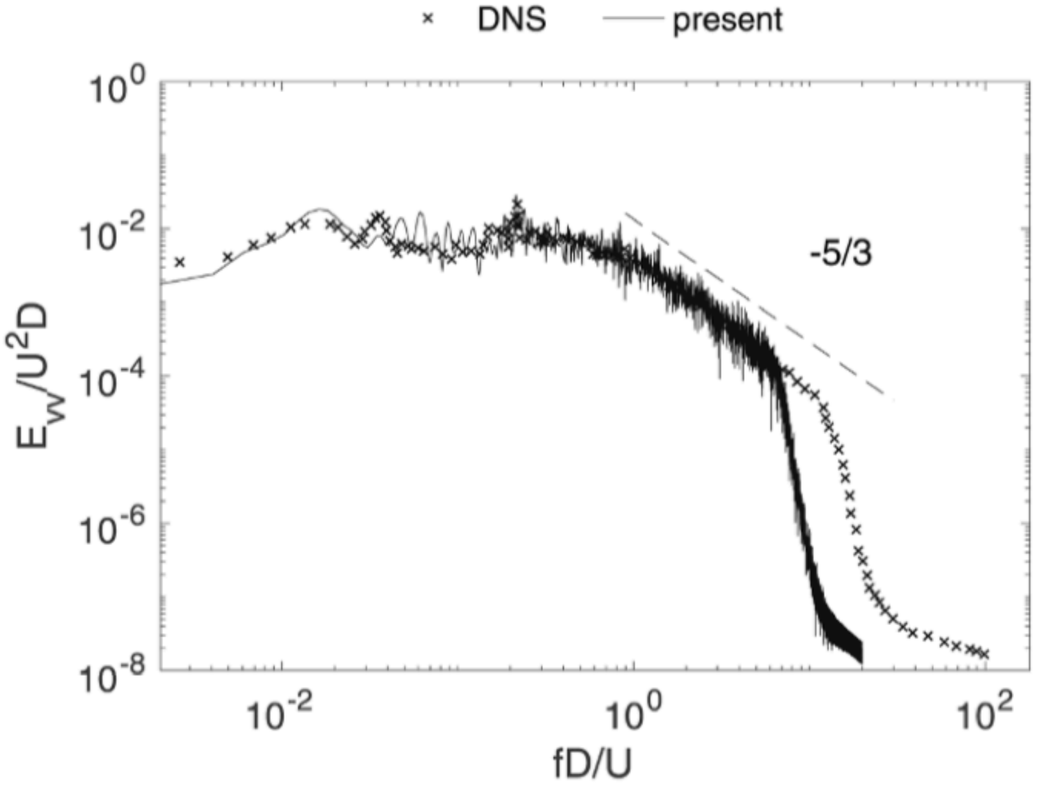
Barcelona Supercomputing Center

Numerics can interact with the SGS model



There is a constant inter-play between numerics and the theoretical dissipation coming from the SGS model





Barcelona Supercomputing Center

Low dissipation NS discretisation with FEM

$$\partial_t \mathbf{u} + (\mathbf{u}\cdot\nabla)\mathbf{u} - \nabla\cdot(2\nu\boldsymbol{\varepsilon}(\mathbf{u})) + \nabla p = \mathbf{f} \qquad \text{in } \Omega\times(t_0,t_f),$$

$$\nabla\cdot\mathbf{u} = 0 \qquad \text{in } \Omega\times(t_0,t_f),$$

$$(\partial_t \mathbf{u},\mathbf{v}) + (\mathbf{u}\cdot\nabla\mathbf{u},\mathbf{v}) + 2\,(\nu\boldsymbol{\varepsilon}(\mathbf{u}),\boldsymbol{\varepsilon}(\mathbf{v})) - (p,\nabla\cdot\mathbf{v}) + (q,\nabla\cdot\mathbf{u}) = (\mathbf{f},\mathbf{v})$$

$$C_{nonc}(\mathbf{u}) = (\mathbf{u}\cdot\nabla)\mathbf{u}$$

$$C_{skew}(\mathbf{u}) = (\mathbf{u}\cdot\nabla)\mathbf{u} + \frac{1}{2}(\nabla\cdot\mathbf{u})\,\mathbf{u}$$

$$C_{emac}(\mathbf{u}) = 2\mathbf{u}\cdot\boldsymbol{\varepsilon}(\mathbf{u}) + (\nabla\cdot\mathbf{u})\,\mathbf{u} - \frac{1}{2}\nabla|\mathbf{u}|^2$$

Energy	Momentum	Angular
-	-	-
X	-	-
X	X	X

*Sergey Charnyi, Timo Heister, Maxim A. Olshanskii, Leo G. Rebholz, *On conservation laws of Navier-Stokes Galerkin discretizations*, JCP, 2017.

Barcelona Supercomputing Center

Low dissipation NS discretisation with FEM

$$(\partial_t \mathbf{u}_h, \mathbf{v}_h) + (C_{emac}(\mathbf{u}_h), \mathbf{v}_h) + \nu(\nabla \mathbf{u}_h, \nabla \mathbf{v}_h) - (p_h, \nabla \cdot \mathbf{v}_h) + (q_h, \nabla \cdot \mathbf{u}_h) = (\mathbf{f}, \mathbf{v}_h)$$

$$\mathsf{M}\partial_t \mathsf{U} + \mathsf{K}(\mathsf{U})\,\mathsf{U} + \mathsf{G}\mathsf{P} = \mathsf{R_m},$$

$$\mathsf{D}\mathsf{U} = \mathsf{R_c},$$

$$\mathsf{M}_{ij}^{ab} = \left(N^b, N^a\right)\delta_{ij},$$

$$\mathsf{G}_i^{ab} = -\left(N^b, \partial_i N^a\right),$$

$$\mathsf{K}\left(\mathsf{U}^{n+1}\right) = \mathsf{K}_{CONV}(\mathsf{U}) + \mathsf{K}_{VISC}(\mathsf{U}),$$

$$\mathsf{K}_{VISC}\left(\mathsf{U}^{n+1}\right)_{ij}^{ab} = \left(\nu\boldsymbol{\varepsilon}(N^b), \boldsymbol{\varepsilon}(N^a)\right)\delta_{ij},$$

$$\mathsf{K}_{CONV}\left(\mathsf{U}^{n+1}\right)_{ij}^{ab} = \left(\mathbf{u}_h \cdot \nabla N^b, N^a\right)\delta_{ij} + \left(\partial_i N^b u_h^j, N^a\right) + \left((\nabla \cdot \mathbf{u}_h) N^b, N^a\right)\delta_{ij} - \frac{1}{2}\left(\partial_i u_h^j N^b, N^a\right),$$

Lehmkuhl, O., Houzeaux, G., Owen, H., Chrysokentis, G., Rodriguez, I., 2019. A low-dissipation finite element scheme for scale resolving simulations of turbulent flows. JCP 390, 51-65.

Barcelona Supercomputing Center

Low dissipation NS discretisation with FEM

We use explicit RK methods to integrate in time the NS equations:

Substeps from i = 2, .., s

$$\mathsf{U}^{i,*} = \mathsf{U}^{n} + \delta t \mathsf{M}^{-1} \sum_{j=1}^{i} a_{ij} \mathsf{F}^{j},$$

$$\mathsf{D}\mathsf{M}^{-1}\mathsf{G}\left(\Phi^{i}\right) = \frac{1}{c_i \delta t}\left(\mathsf{D}\mathsf{U}^{i,*} - \mathsf{R}_{\mathsf{c}}\right),$$

$$\mathsf{U}^{i} = \mathsf{U}^{i,*} - c_i \delta t \mathsf{M}^{-1}\mathsf{G}\left(\Phi^{i}\right),$$

Final step:

$$\mathsf{U}^{n+1,*} = \mathsf{U}^{n} + \delta t \mathsf{M}^{-1} \sum_{i=1}^{s} b_{i} \mathsf{F}^{i},$$

$$\mathsf{D}\mathsf{M}^{-1}\mathsf{G}\left(\Phi^{n+1}\right) = \frac{1}{\delta t}\left(\mathsf{D}\mathsf{U}^{n+1,*} - \mathsf{R}_{\mathsf{c}}\right),$$

$$\mathsf{U}^{n+1} = \mathsf{U}^{n+1,*} - \delta t \mathsf{M}^{-1}\mathsf{G}\left(\Phi^{n+1}\right),$$

Lehmkuhl, O., Houzeaux, G., Owen, H., Chrysokentis, G., Rodriguez, I., 2019. A low-dissipation finite element scheme for scale resolving simulations of turbulent flows. JCP 390, 51-65.

Barcelona Supercomputing Center

Low dissipation NS discretisation with FEM

The use of the discrete Laplacian, $\mathsf{DM}^{-1}\mathsf{G}$, is relatively expensive even if a diagonal mass matrix is used. Therefore, when continuous pressure interpolations are used, it is usually approximated as

$$\mathsf{DM}^{-1}\mathsf{G} \approx \mathsf{L}, \qquad \text{with components} \quad \mathsf{L}^{ab} = -\left(\nabla N^a, \nabla N^b\right)$$

This introduces and stabilising term of the form:

$$\delta t \mathsf{B}\Phi \text{ where } \mathsf{B} = \mathsf{DM}^{-1}\mathsf{G} - \mathsf{L}$$

Therefore, at the kinetic energy level a dissipation is introduced with the form:

$$\delta t \left(\Phi^{n+1}\right)^{\mathsf{T}} \mathsf{B}\Phi^{n+1}$$



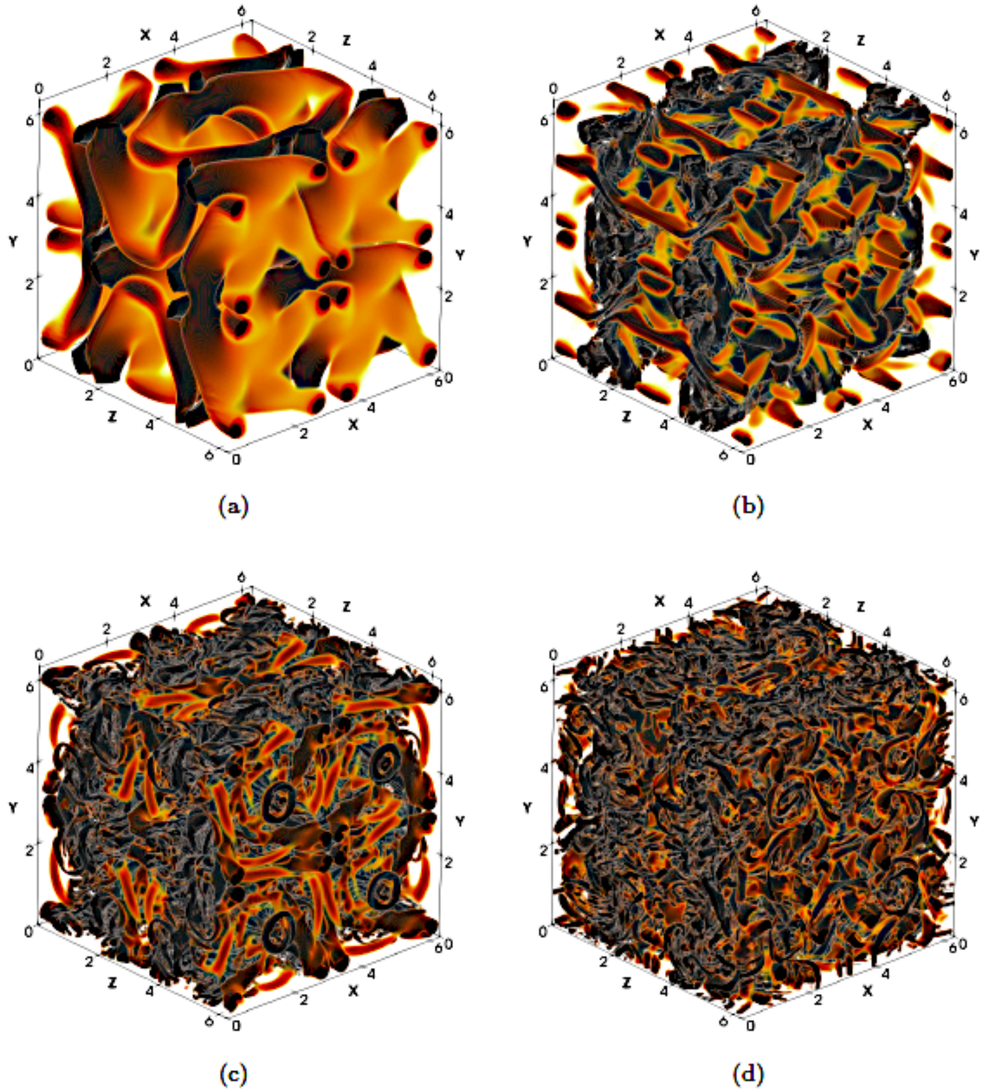
Final dissipation scaling similar to collocated FVM & FD !!

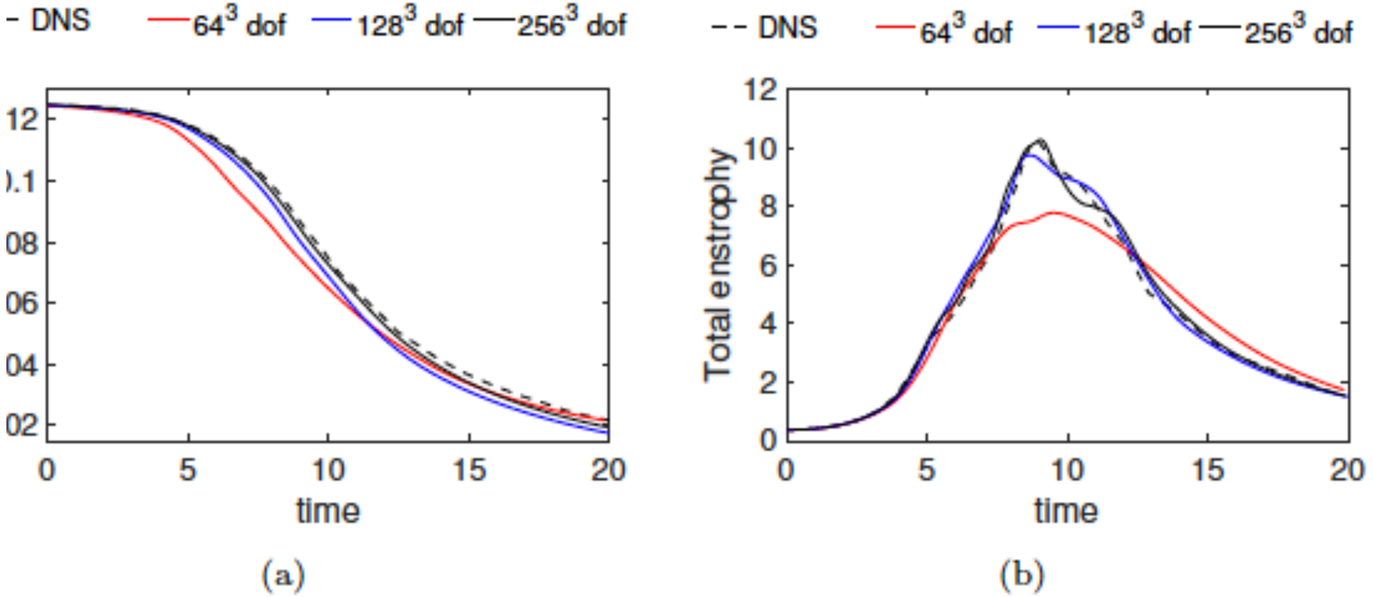
$$\mathcal{O}\left(\delta t\, h^{k+1}\right)$$

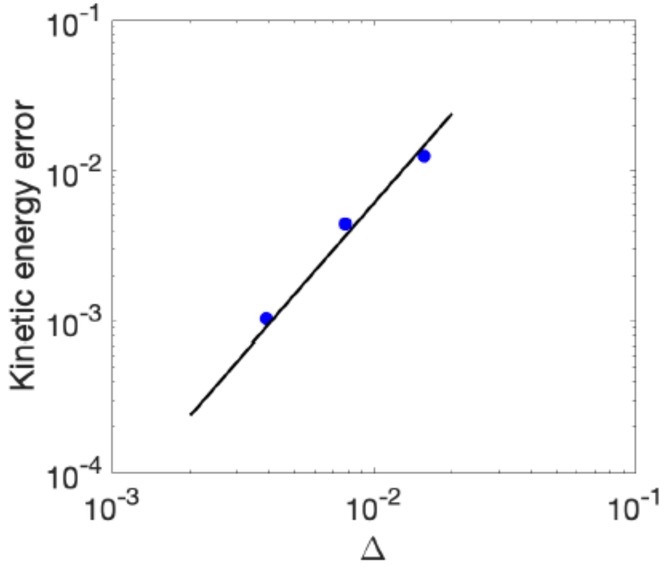
Lehmkuhl, O., Houzeaux, G., Owen, H., Chrysokentis, G., Rodriguez, I., 2019. A low-dissipation finite element scheme for scale resolving simulations of turbulent flows. JCP 390, 51-65.

Barcelona Supercomputing Center

Low dissipation NS discretisation with FEM



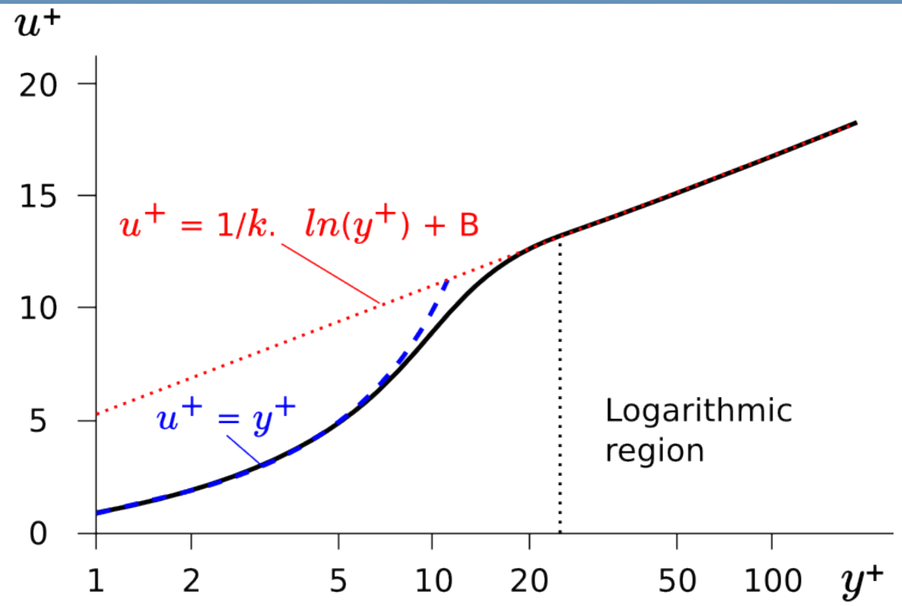




Lehmkuhl, O., Houzeaux, G., Owen, H., Chrysokentis, G., Rodriguez, I., 2019. A low-dissipation finite element scheme for scale resolving simulations of turbulent flows. JCP 390, 51-65.

Barcelona Supe

Scales at the wall are case dependent: wall modelled LES

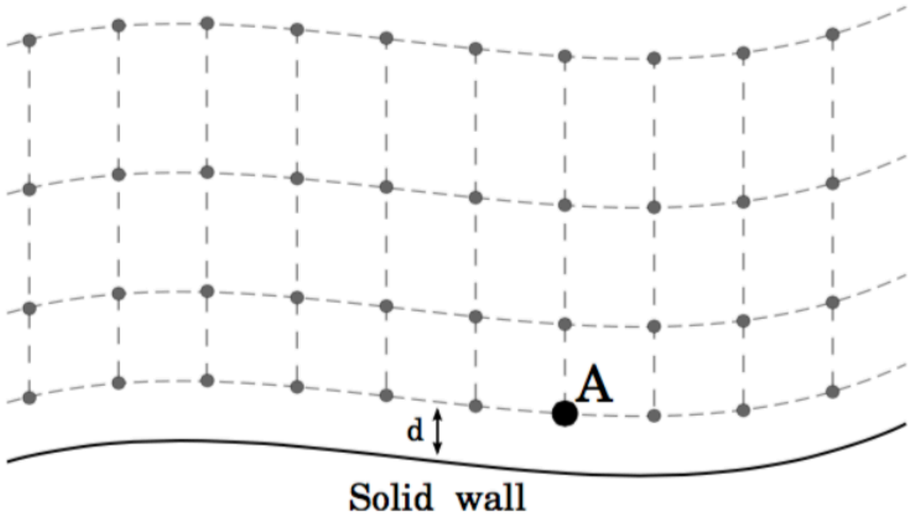




Schematic illustrating a typical wall-modeled grid resolution, chosen to resolve the energetic eddies in the outer portion of the boundary layer, whose size scales with δ. Contours visualized represent the instantaneous streamwise velocity in a turbulent channel flow (Reτ = 4,200). The contours range from U + = 6 (blue) to 18 (white). Data taken from the direct numerical simulation of Lozano-Duran & Jimenez (2014); Figure taken from Bose and Park (2018);

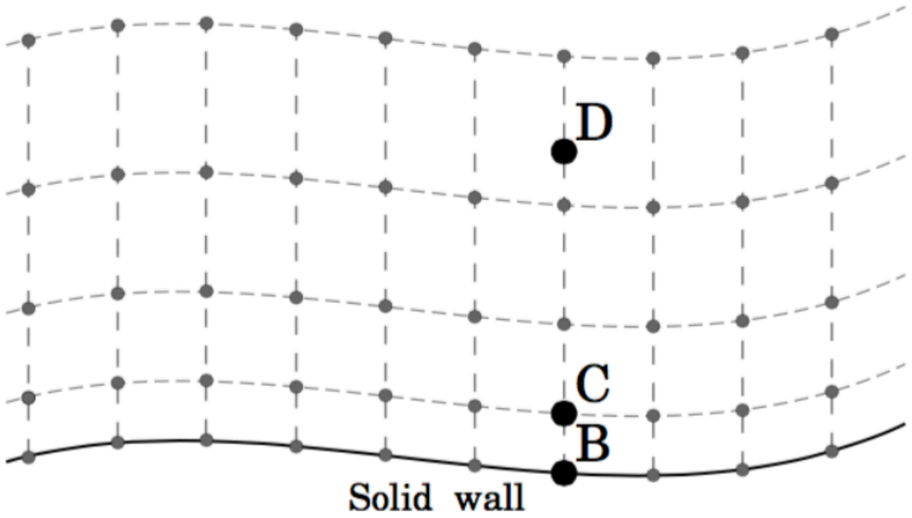
Barcelona Supercomputing Center

Scales at the wall are case dependent: wall modelled LES



Standard FE approach

D within the inner portion of the boundary layer



B-C Standard FD

B-D Exchange location (Kawai & Larsson)

C or D Time Filtering (Yang et al.)

- Between point B and D the wall model is used
  - A simple equilibrium model can be used by means of analytical solutions.
  - An extra domain solving B to D with 3D RANS equations can be also added in order to take into-account non-equilibrium effects.
- In point B wall shear stress is imposed in the LES domain.

Barcelona Supercomputing Center

Scales at the wall are case dependent: wall modelled LES

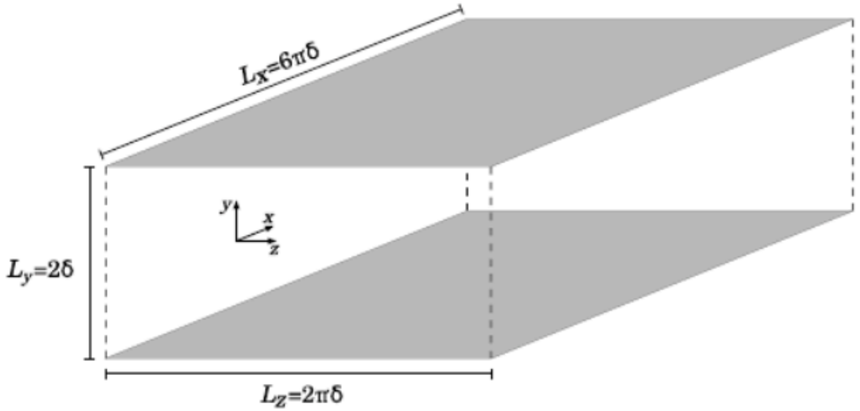
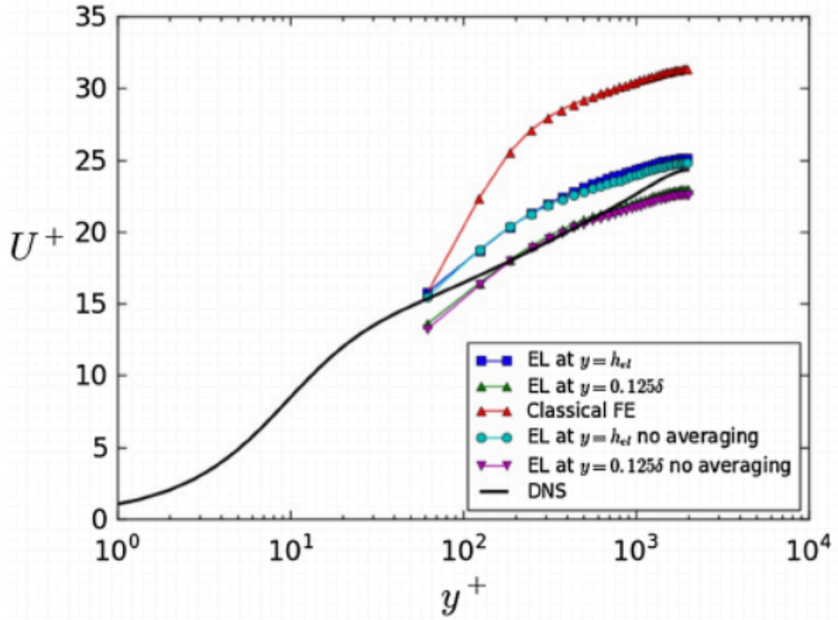
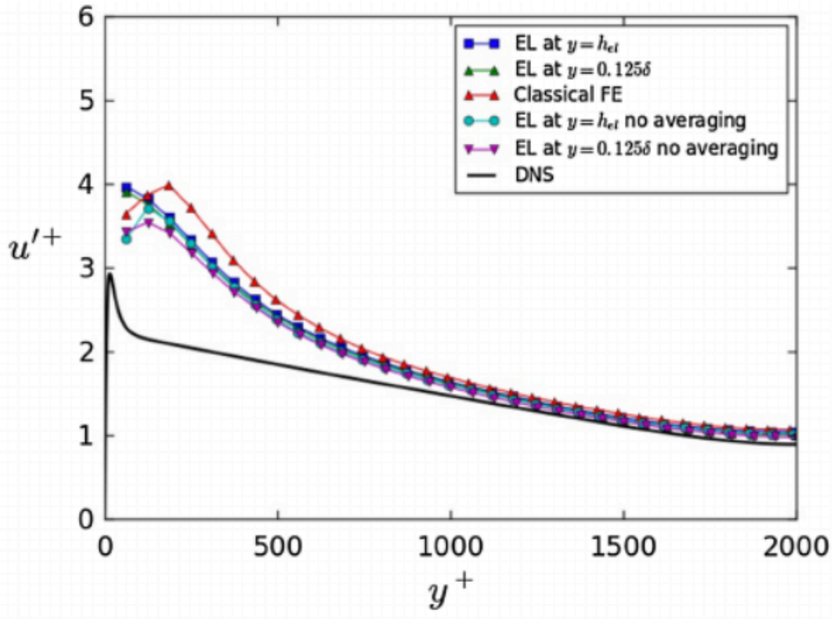


FIGURE 3 Computational domain for the turbulent channel case
[Colour figure can be viewed at wileyonlinelibrary.com]



(A) *Mean streamwise velocity*

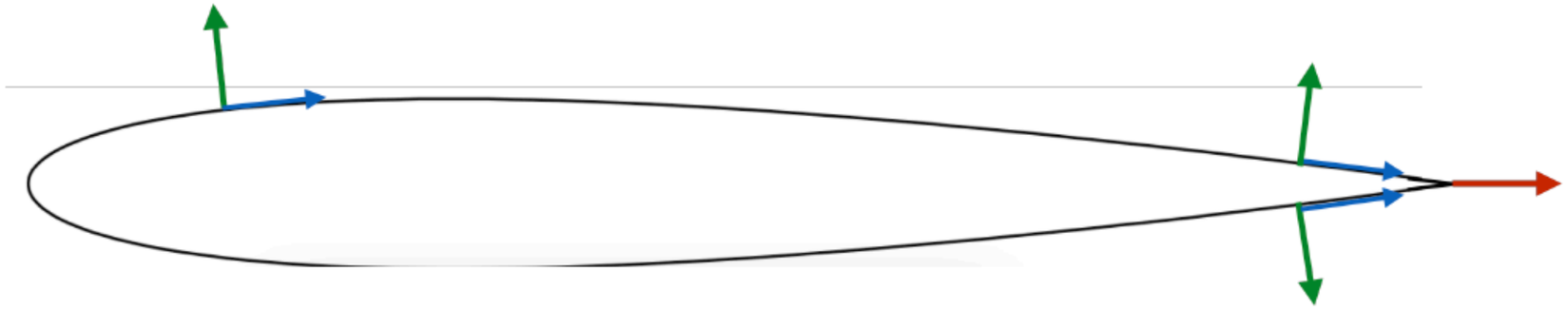


(B) *Rms streamwise velocity fluctuation*

Barcelona Supercomputing Center

Owen, H, Chrysokentis, G, Avila, M, et al. Wall-modeled large-eddy simulation in a finite element framework. *Int J Numer Meth Fluids*. 2020; 92: 20– 37. https://doi.org/10.1002/fld.4770

Scales at the wall are case dependent: wall modelled LES



Artificial stagnation at trailing edge

Solution

Free velocity

Disadvantages

- Non zero flow through boundary
- Nearly imposible to do in complex geometries

Similar problems appear in the top edge of a Backward Facing Step

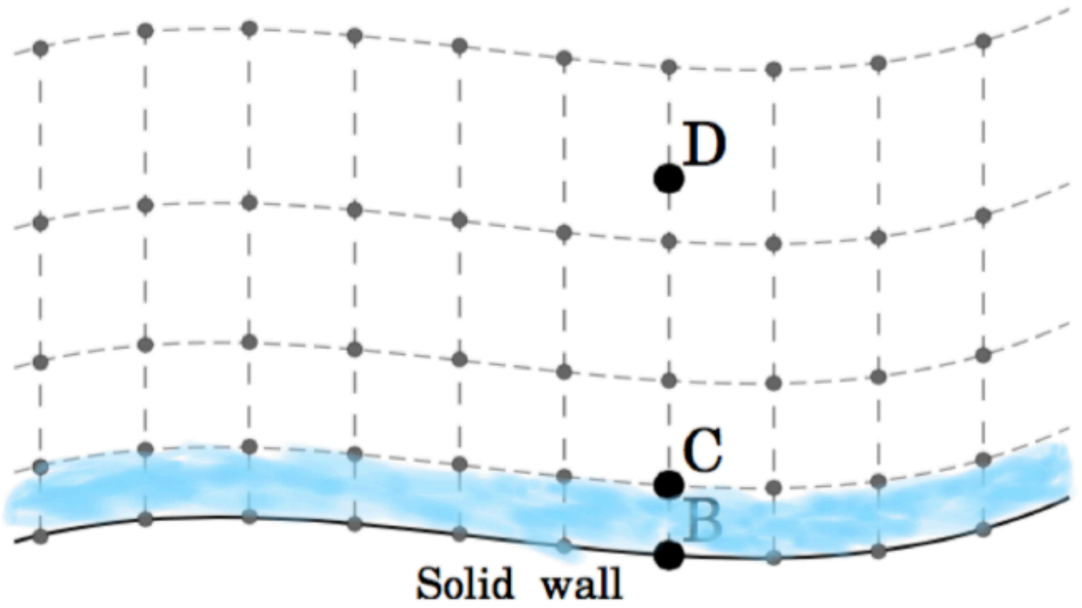
"A Finite-element Viscosity Based Non-slip Wall Modelling Strategy for the Simulation of Industrial Turbulent Flows.", H. Owen, S. Radhakrishnan, S. Gomez and O. Lehmkuhl, ERCOFTAC Bulletin 120, pages. 61-66, September 2019.

Barcelona Supercomputing Center

Scales at the wall are case dependent: wall modelled LES

Set the velocity to zero at the wall
and
modify the viscosity in the first element such that

$$\tau = \mu_{first-element} \frac{\partial u_t}{\partial n}$$



- Traction from wall law input — input instantaneous or average velocity at exchange location (C or D)
- Tangential velocity gradient in the normal direction
- We thus obtain the viscosity to be used in the first element.

"A Finite-element Viscosity Based Non-slip Wall Modelling Strategy for the Simulation of Industrial Turbulent Flows.", H. Owen, S. Radhakrishnan, S. Gomez and O. Lehmkuhl, ERCOFTAC Bulletin 120, pages. 61-66, September 2019.

Barcelona Supercomputing Center

Scales at the wall are case dependent: wall modelled LES

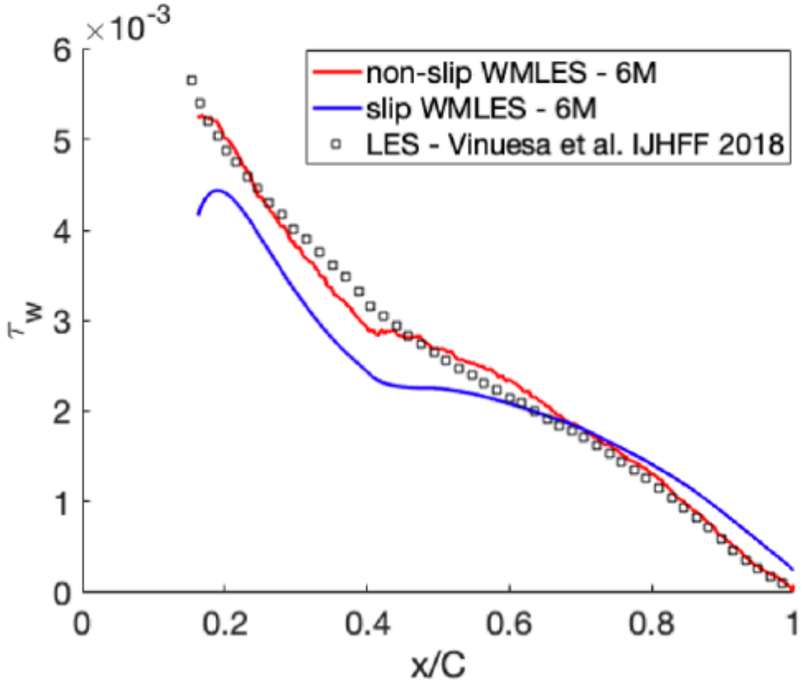


Figure 4: NACA4412 at $Re_c = 10^6$ and $AoA = 5^o$. Wall shear stress at the suction side, WMLES results vs wall resolved results from Vinuesa et al. [23].

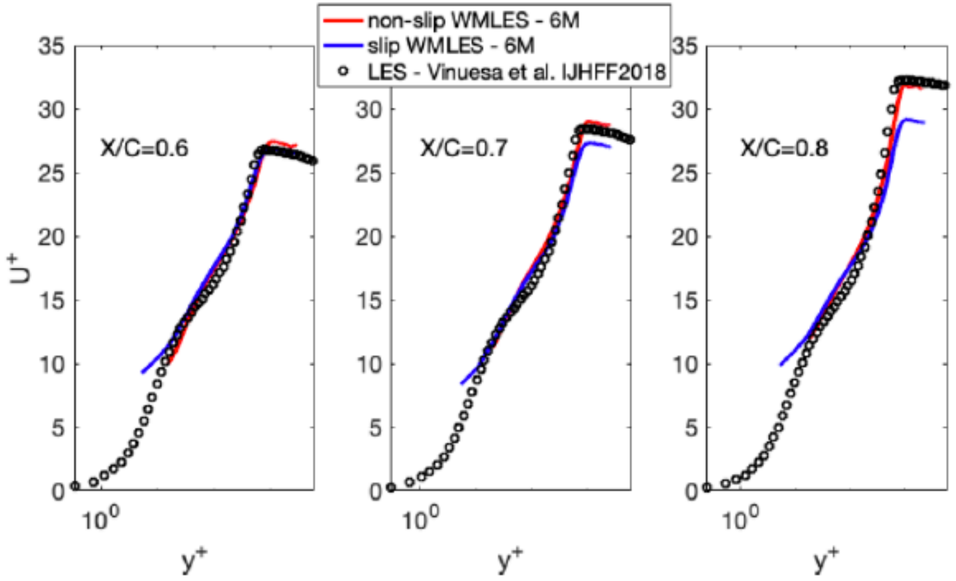


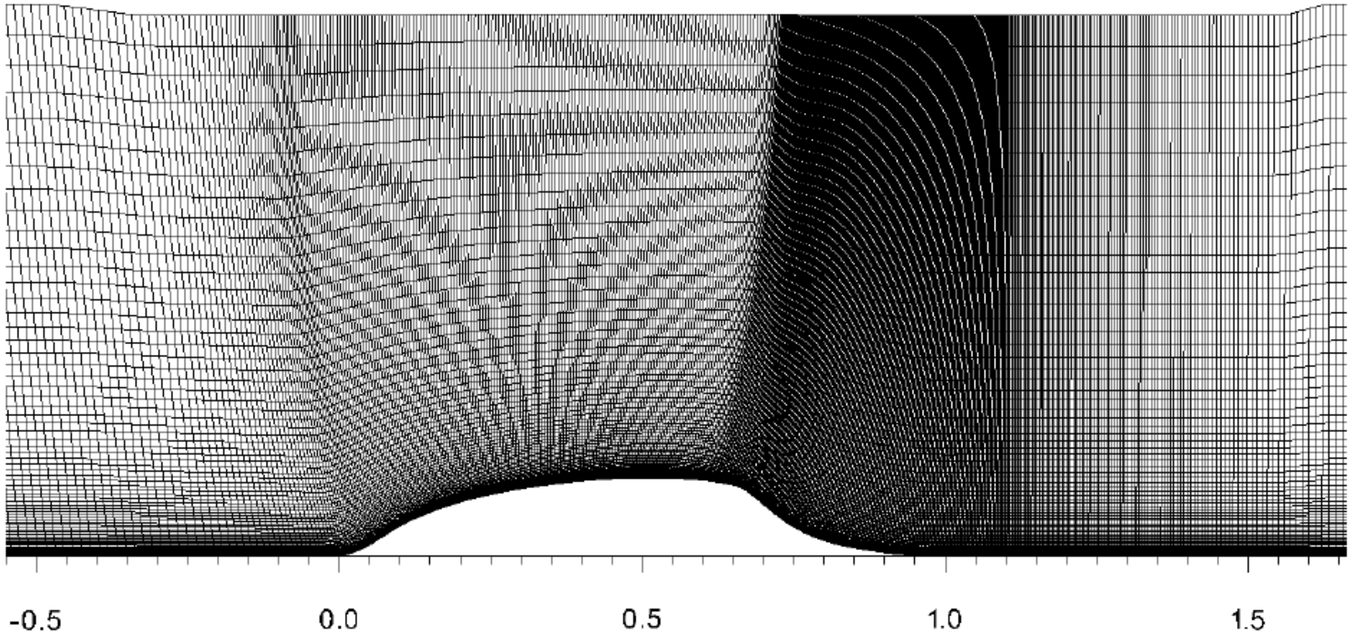
Figure 5: NACA4412 at $Re_c = 10^6$ and $AoA = 5^o$. Mean velocity profiles in wall units at position x/C = 0.6, 0.7 and 0.8, WMLES results vs wall resolved LES results from Vinuesa et al. [23].

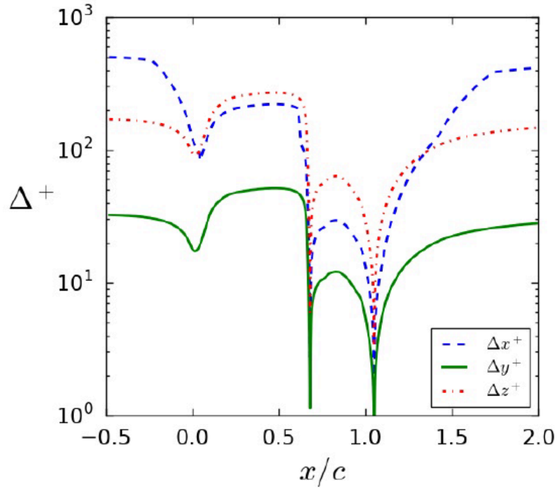
"A Finite-element Viscosity Based Non-slip Wall Modelling Strategy for the Simulation of Industrial Turbulent Flows.", H. Owen, S. Radhakrishnan, S. Gomez and O. Lehmkuhl, ERCOFTAC Bulletin 120, pages. 61-66, September 2019.

Barcelona Supercomputing Center

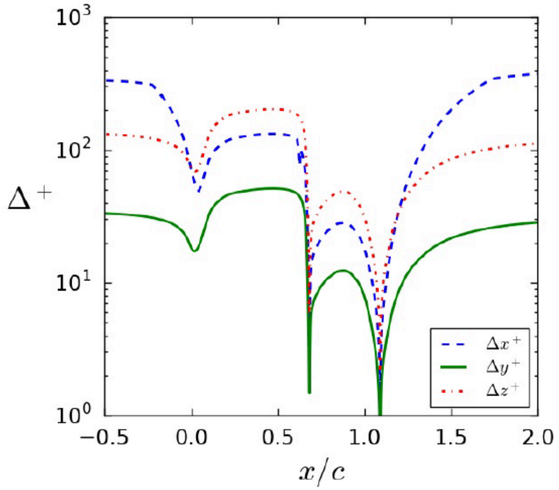
Scales at the wall are case dependent: exchange location

Flow over a wall-mounted hump at Re = 936000, 3M & 8M elements mesh





(a) *Coarse grid (G1)*

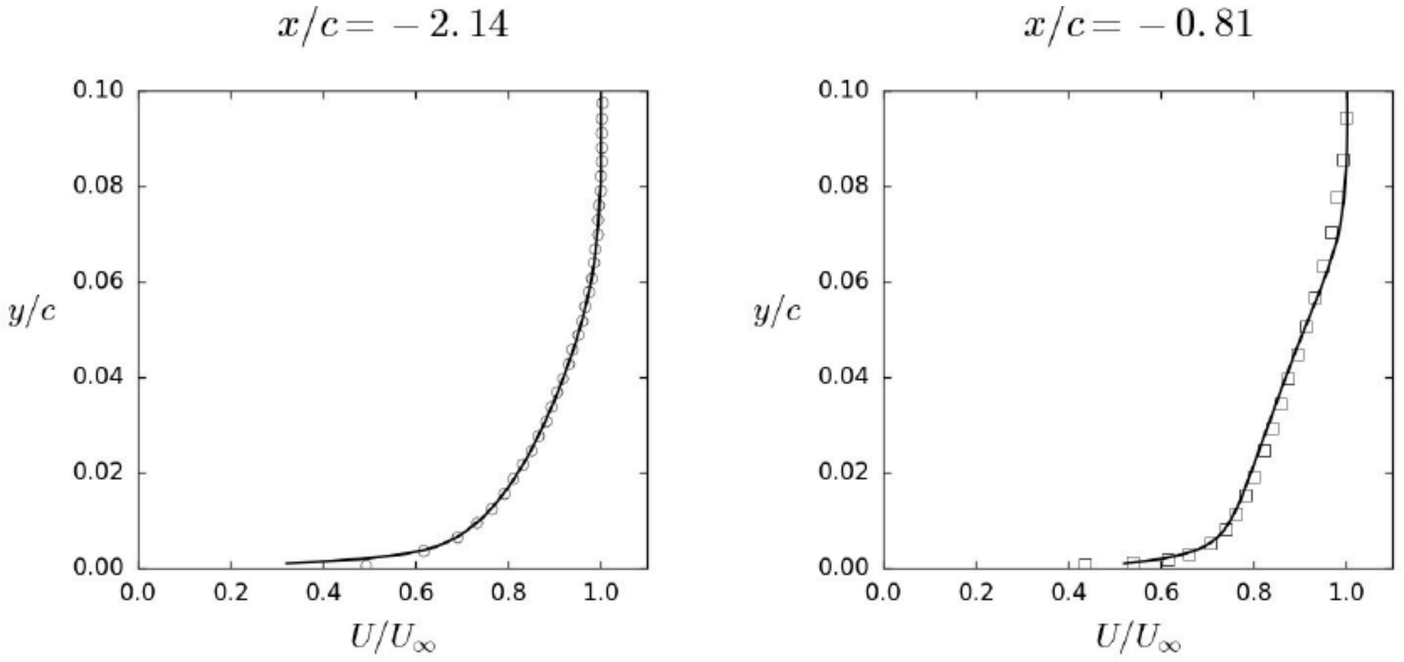


(b) *Fine grid (G2)*

Barcelona Supercomputing Center

Scales at the wall are case dependent: exchange location

Flow over a wall-mounted hump at Re = 936000, 3M & 8M elements mesh

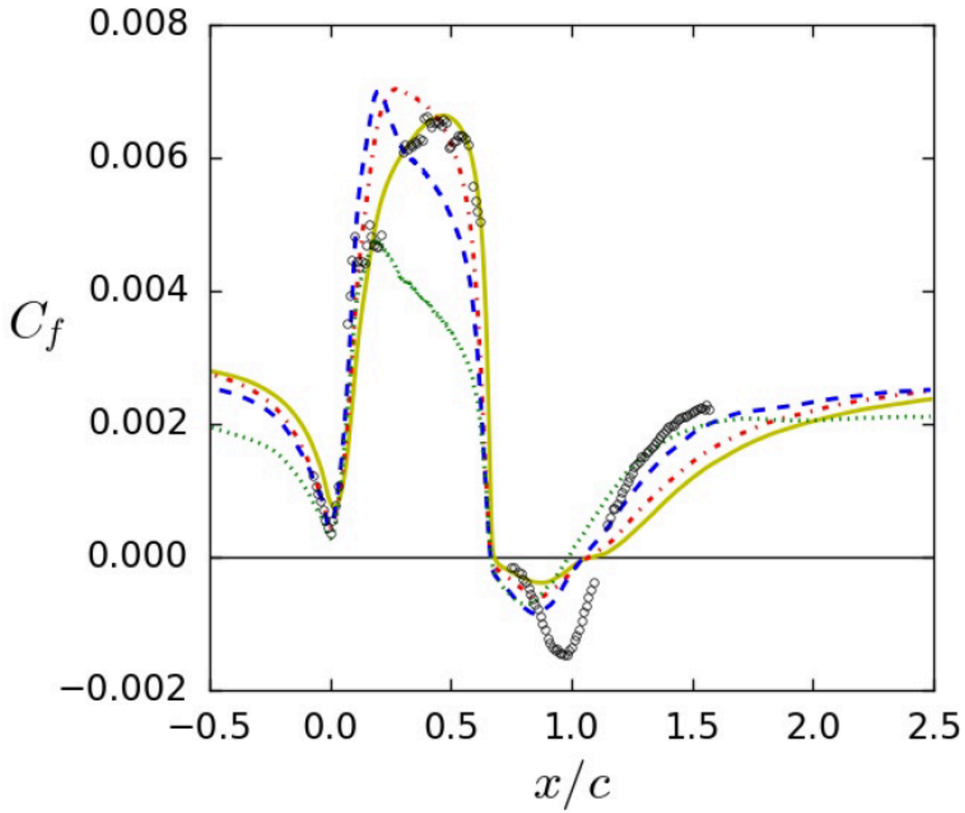


Simulation	x_{sep}/c G1	x_{reatt}/c G1	$(x_{reatt})_{error}$ G1	x_{sep}/c G2	x_{reatt}/c G2	$(x_{reatt})_{error}$ G2
Classical FE	0.665	0.97	11.8%	0.665	0.985	10.5%
EL at 1st point	0.665	0.99	10.0%	0.665	1.05	4.5%
EL at 3rd point	0.665	1.03	6.3%	0.665	1.07	2.7%
EL at $h = 0.125\delta_{in}$	0.67	1.05	4.5%	0.67	1.09	0.9%
Experiment	~ 0.665	~ 1.1	-			

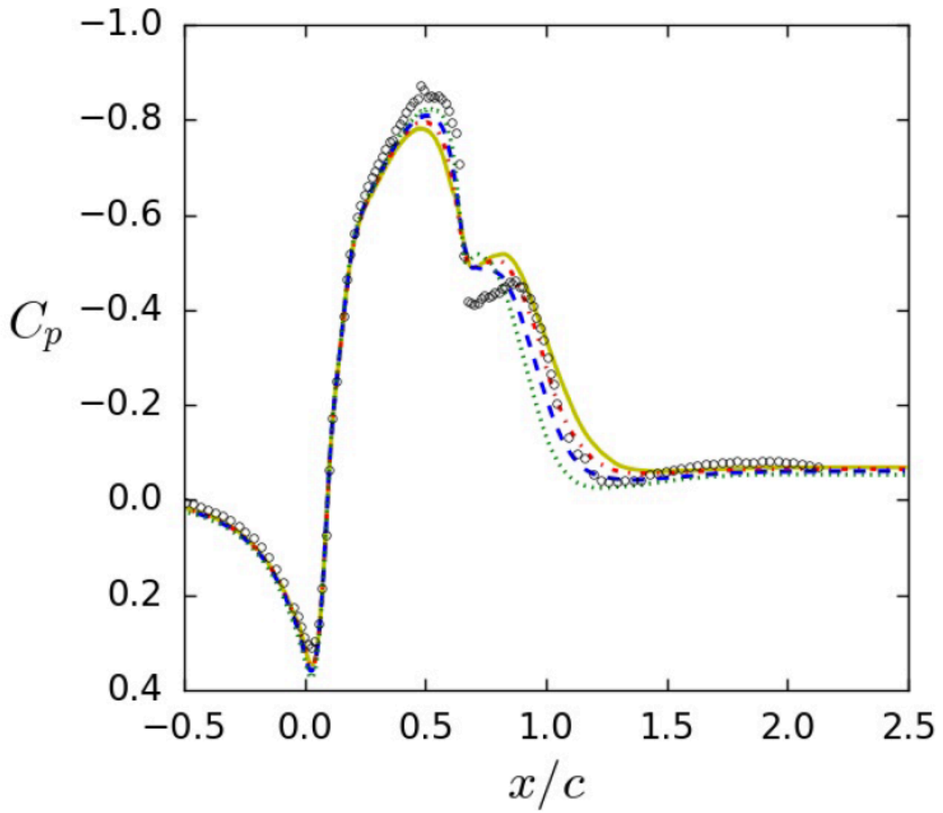
Barcelona Supercomputing Center

Scales at the wall are case dependent: exchange location

Flow over a wall-mounted hump at Re = 936000, 3M & 8M elements mesh



(a) *Skin friction coefficient*



(b) *Pressure coefficient*

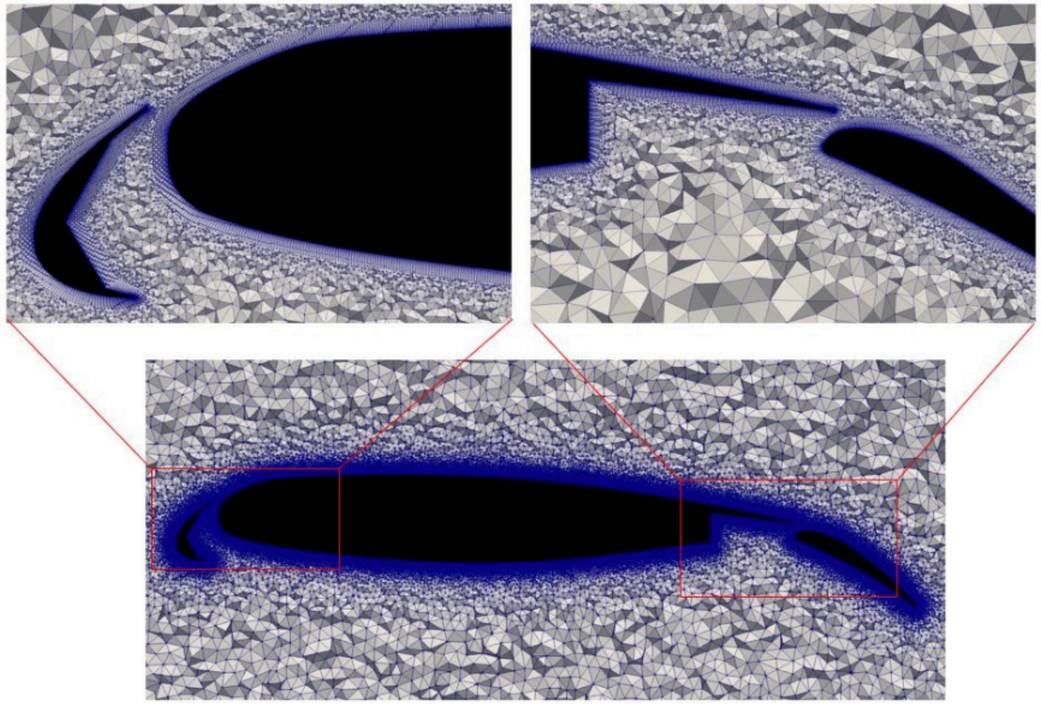
Figure 9: Skin friction (a) and pressure (b) coefficients across the streamwise direction. Green dotted line: classic FE method, blue dashed line: exchange location at first grid point, red dash-dotted line: exchange location at third grid point, yellow solid line: exchange location at $y = 0.125\delta$, circles: experiment (Greenblatt et al [28]).

Barcelona Supercomputing Center

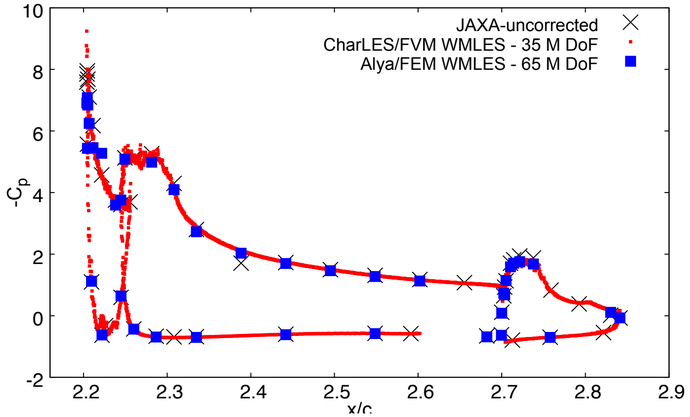
JAXA High-lift: previous validation

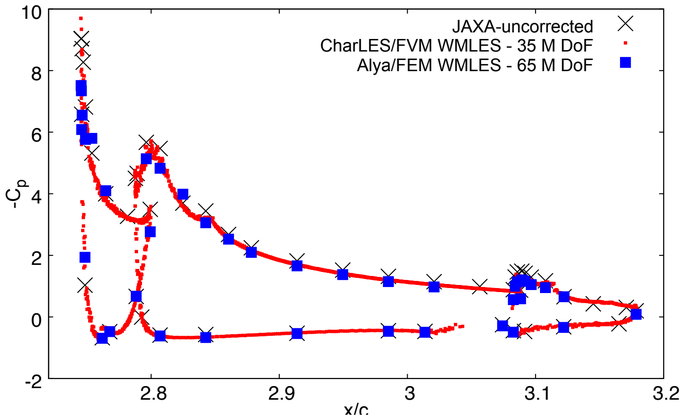
- JAXA high lift in freestream conditions.
- Re = 1.93 M and Ma = 0.172
- AoA = 10, 18.58 and 21.57º
- Vreman SGS model and eq. wall model.

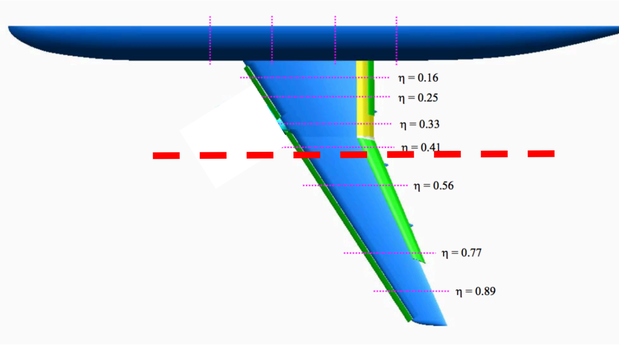
AoA = **18.5º**

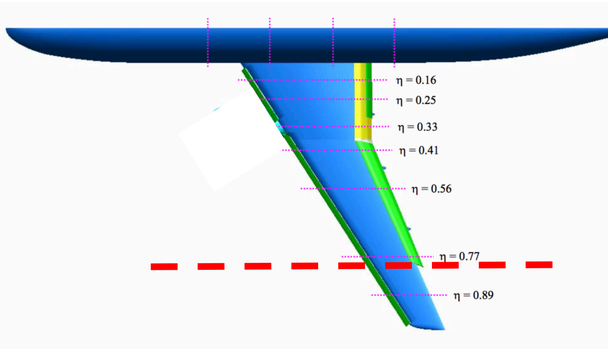


(b) Hybrid grid usede in the Alya calculations, showing prismatic refinement windows near solid boundaries blended with farfield tetrahedra.



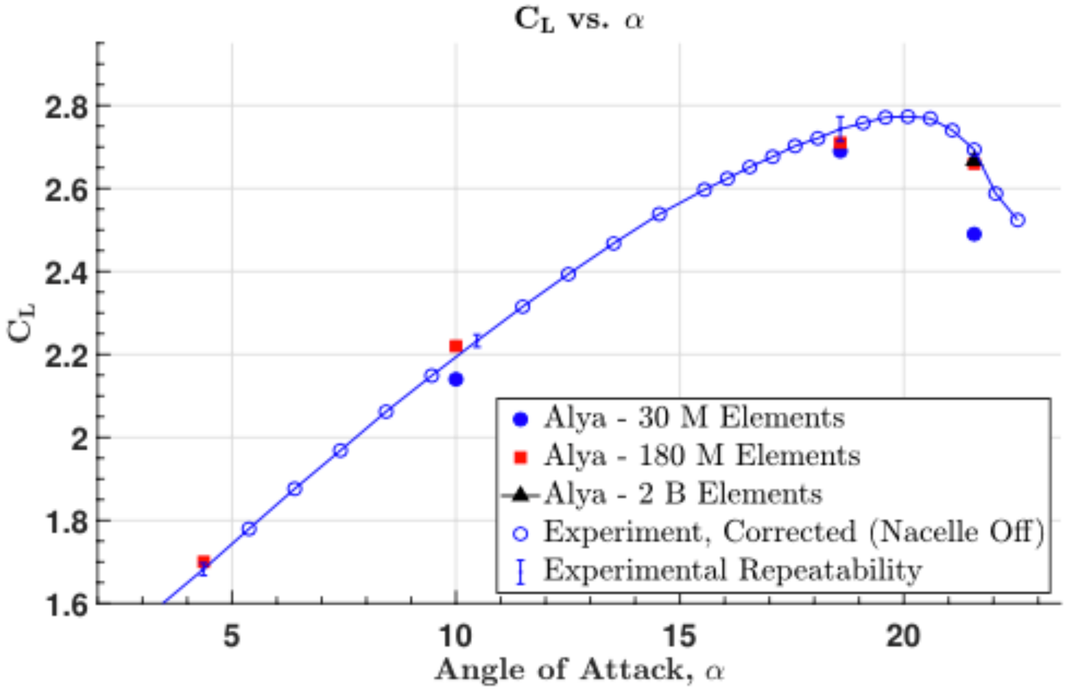




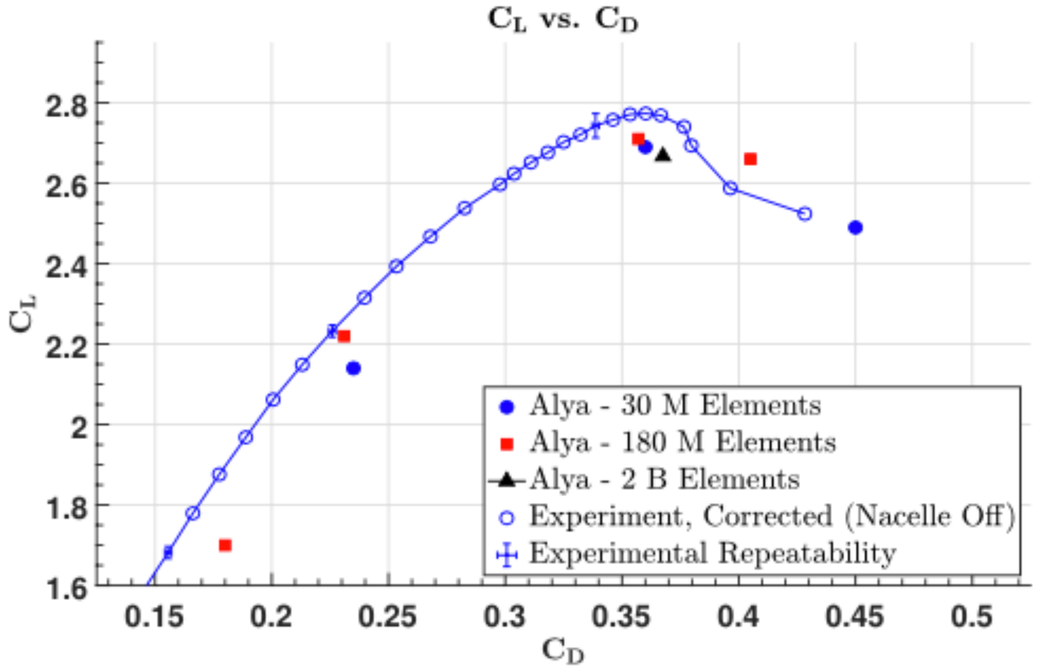


*Lehmkuhl, Park, Bose and Moin. ***Large-eddy simulation of practical aeronautical flows at stall conditions***, Proceedings of the summer program 2018, Center for Turbulence Research, Stanford.

JAXA High-lift: previous validation



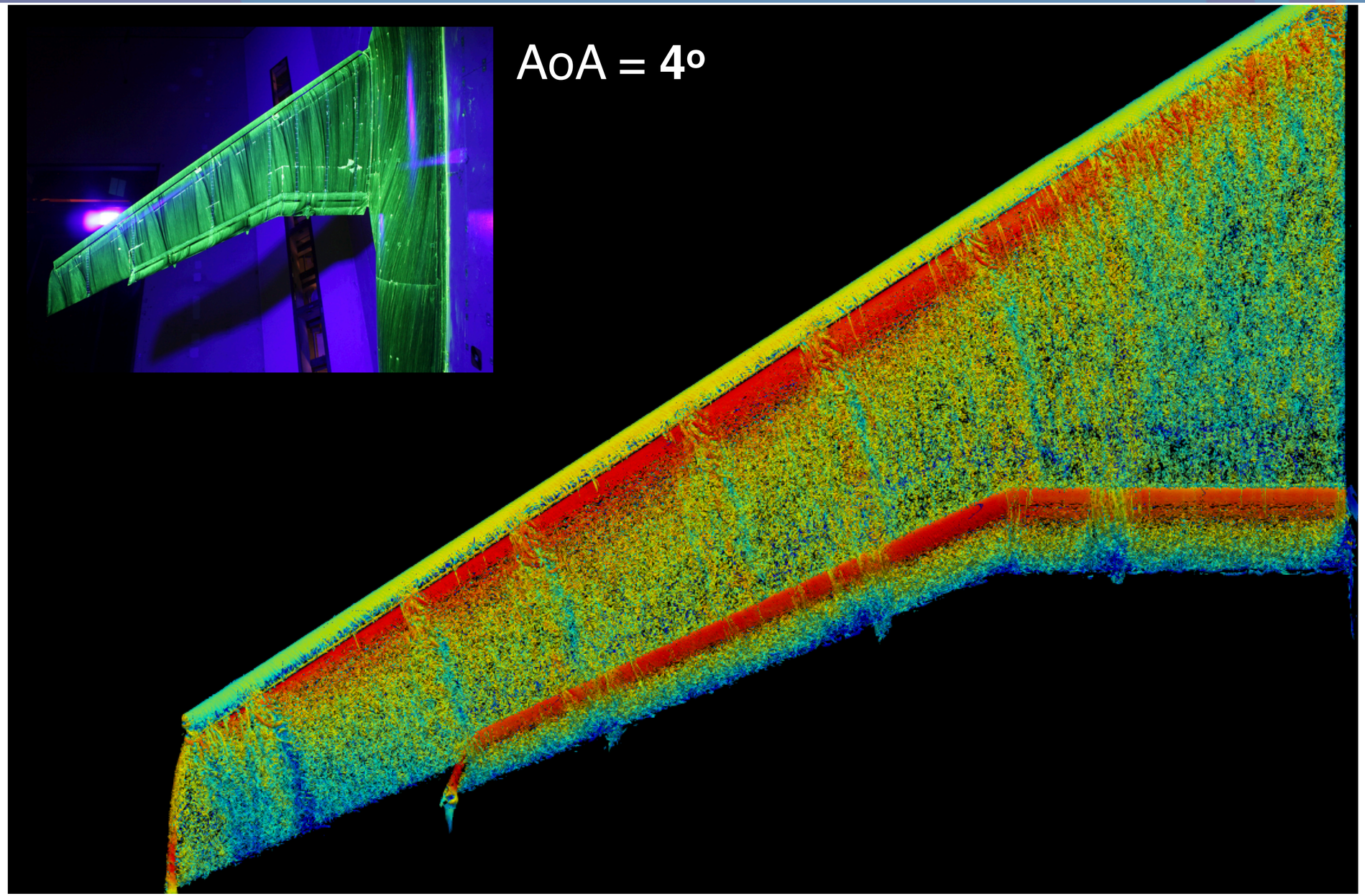
(a) Grid refinement using Alya finite element code.



(a) Grid refinement using Alya finite element code.

Collaboration with: K.A. Goc, G. I. Park, S.T. Bose and P. Moin

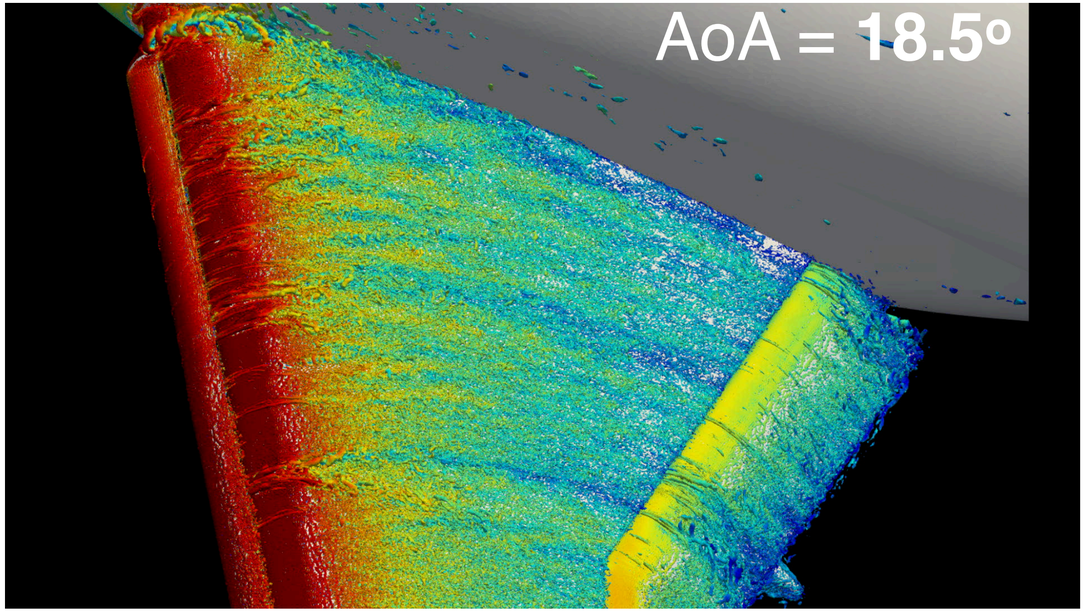
wmLES of massively separated aircraft wake (CTR SP 2018)

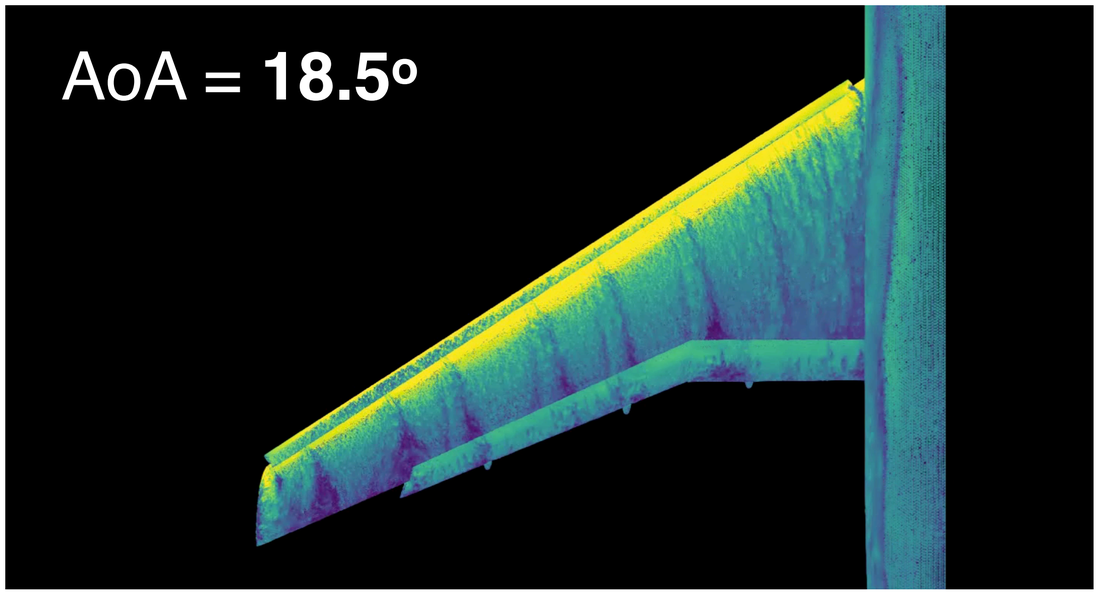


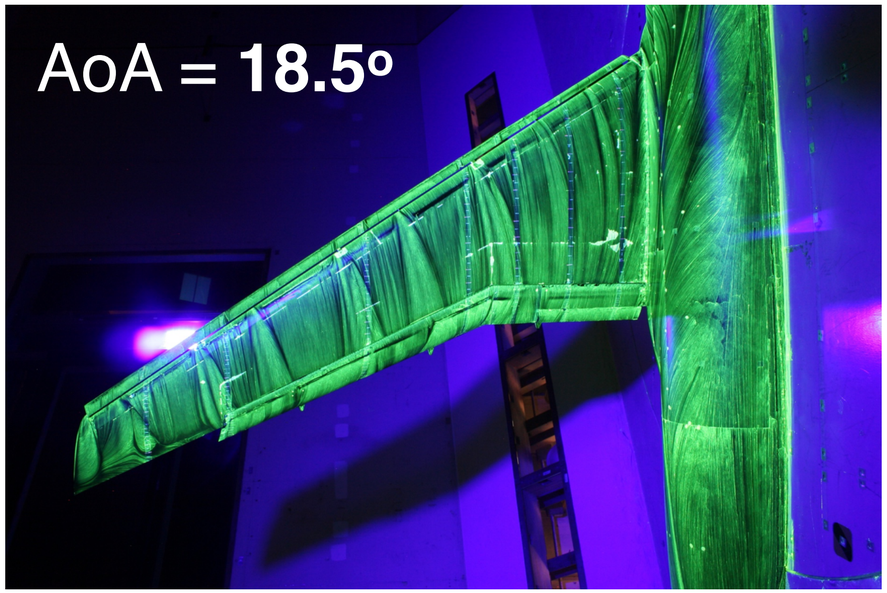
Collaboration with: K.A. Goc, G. I. Park, S.T. Bose and P. Moin

Barcelona Supercomputing Center

wmLES of massively separated aircraft wake (CTR SP 2018)





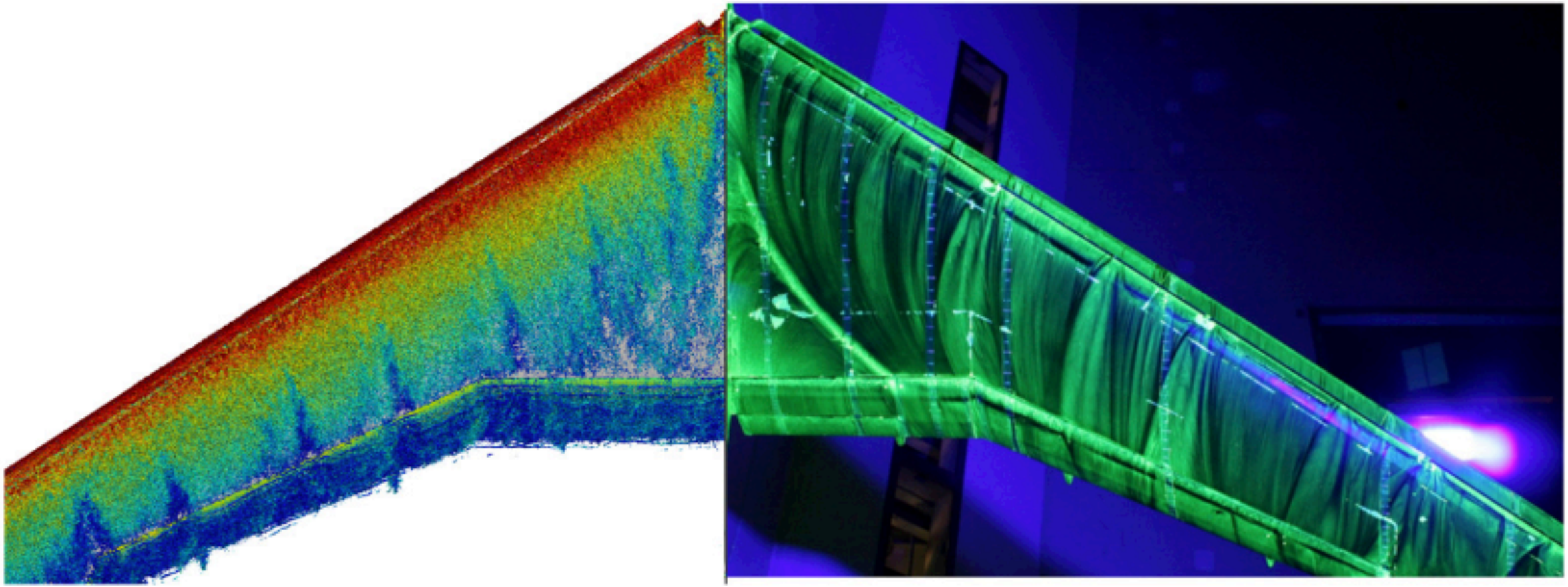


Collaboration with: K.A. Goc, G. I. Park, S.T. Bose and P. Moin

Barcelona Supercomputing Center

wmLES of massively separated aircraft wake (CTR SP 2018)

AoA = **21.5º**



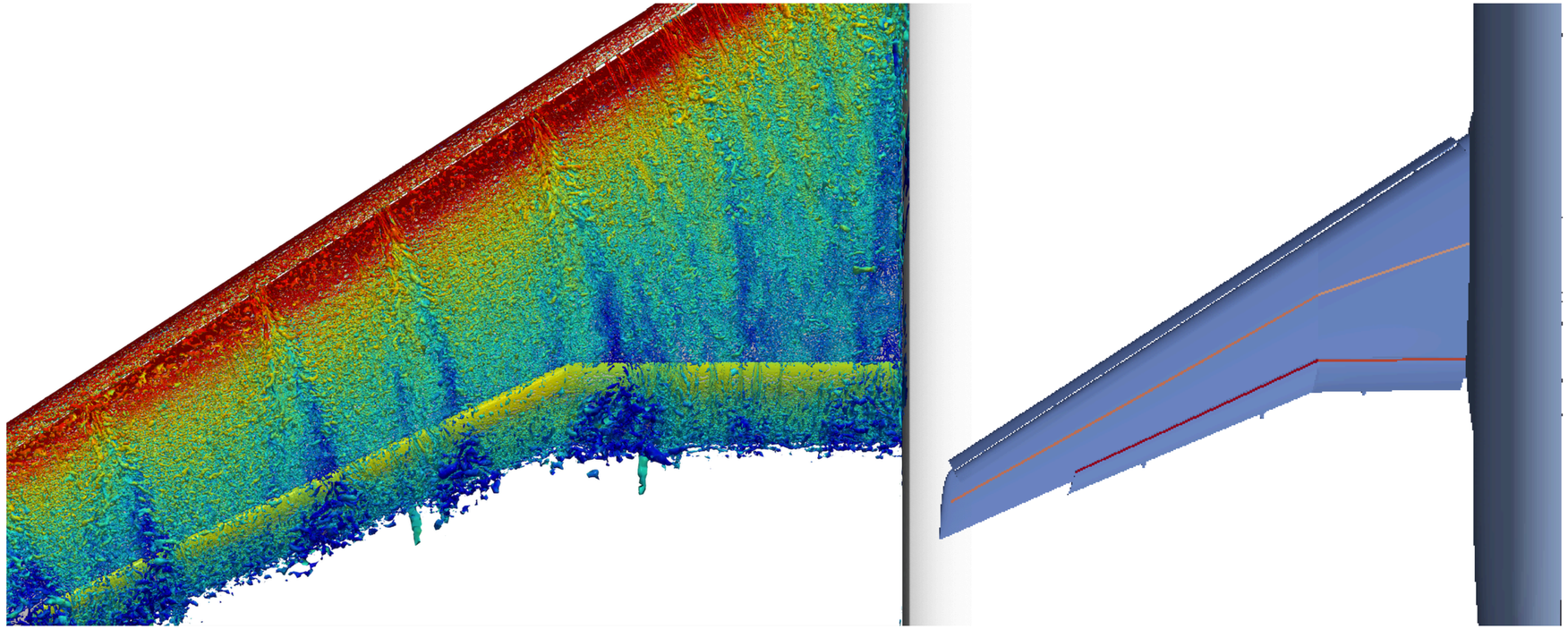
The 2B mesh is still lacking the correct separation!

Collaboration with: K.A. Goc, G. I. Park, S.T. Bose and P. Moin

Barcelona Supercomputing Center

JAXA High-lift AFC parameters

$$F^+ = f_{act} C / U_{ref} \qquad c_\mu = \frac{(\rho V_{max}^2) A_{act}}{(\rho V_{ref}^2) A_{ref}} \qquad \vec{V} = \vec{V}_{max} \sin(2\pi f t) \sin(2\pi \tau_y y)$$



	Act. Loc. x/C
Main	0.5
Flap	0.1

Collaboration with: Adrian Lozano Duran and Ivette Rodriguez

EXCELLERAT

JAXA High-lift AFC parameters

Case		Φ[deg]	C_μ	F^+	3D/2D
AFC1	Main	0	0.015	1.52	3D
	Flap	0			
AFC2	Main	-	-	-	-
	Flap	0	0.015	1.52	3D
AFC3	Main	0	0.0075	1.52	3D
	Flap	0	0.0015		
AFC4	Main	-	-	-	-
	Flap	0	0.0015	1.52	3D
AFC5	Main	60	0.0075	1.52	2D
	Flap	0	0.0015		3D
AFC6	Main	60	0.015	1.52	2D
	Flap	0	0.0015		3D
AFC7	Main	60	0.0075	1.52	3D
	Flap	0	0.0015		
AFC8	Main	45	0.015	1.52	2D
	Flap	0	0.0015		3D
AFC9	Main	45	0.015	15.2	2D
	Flap	0	0.0015		3D
AFC10	Main	45	0.015/0.023	1.52	2D
	Flap	0	0.0015		3D

Collaboration with: Adrian Lozano Duran and Ivette Rodriguez

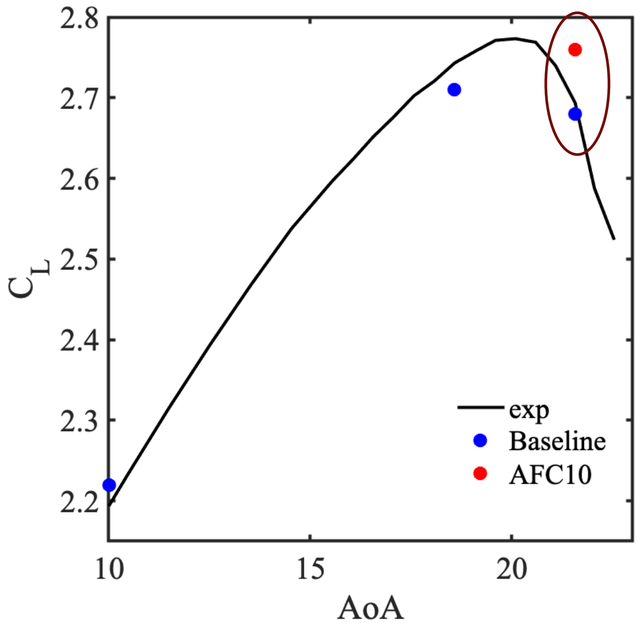
JAXA High-lift AFC results

		C_L	C_D	C_L/C_D	C_{Lrms}	C_{Drms}
	Baseline	2.685	0.405	6.630	0.004	0.002
Φ[deg] = 0 °	AFC1	2.574(-4.1%)	0.365 (10.1%)	7.056 (6.4%)	0.059	0.012
	AFC2	2.595(-3.4%)	**0.359 (11.4%)**	**7.226 (9.0%)**	0.046	0.011
	AFC3	2.668(-0.6%)	0.382 (5.7%)	6.980 (5.3%)	0.024	0.006
	AFC4	2.689(0.1%)	0.380 (6.2%)	7.080 (6.8%)	0.012	0.005
Φ[deg] = 60 °	AFC5	2.695(0.4%)	0.380 (6.2%)	**7.096 (7.0%)**	0.051	0.023
	AFC6	2.719(1.3%)	0.385 (4.9%)	7.072 (6.7%)	0.063	0.029
	AFC7	2.685	0.380 (6.2%)	7.075 (6.7%)	0.015	0.005
Φ[deg] = 45 °	AFC8	2.722(1.4%)	0.390 (3.7%)	6.979 (5.3%)	0.091	0.042
	AFC9	2.711(1.0%)	0.385 (4.9%)	7.047 (6.3%)	**0.811**	**0.360**
	AFC10	**2.754(2.6%)**	0.391 (3.5%)	7.040 (6.2%)	0.112	0.051

Collaboration with: Adrian Lozano Duran and Ivette Rodriguez

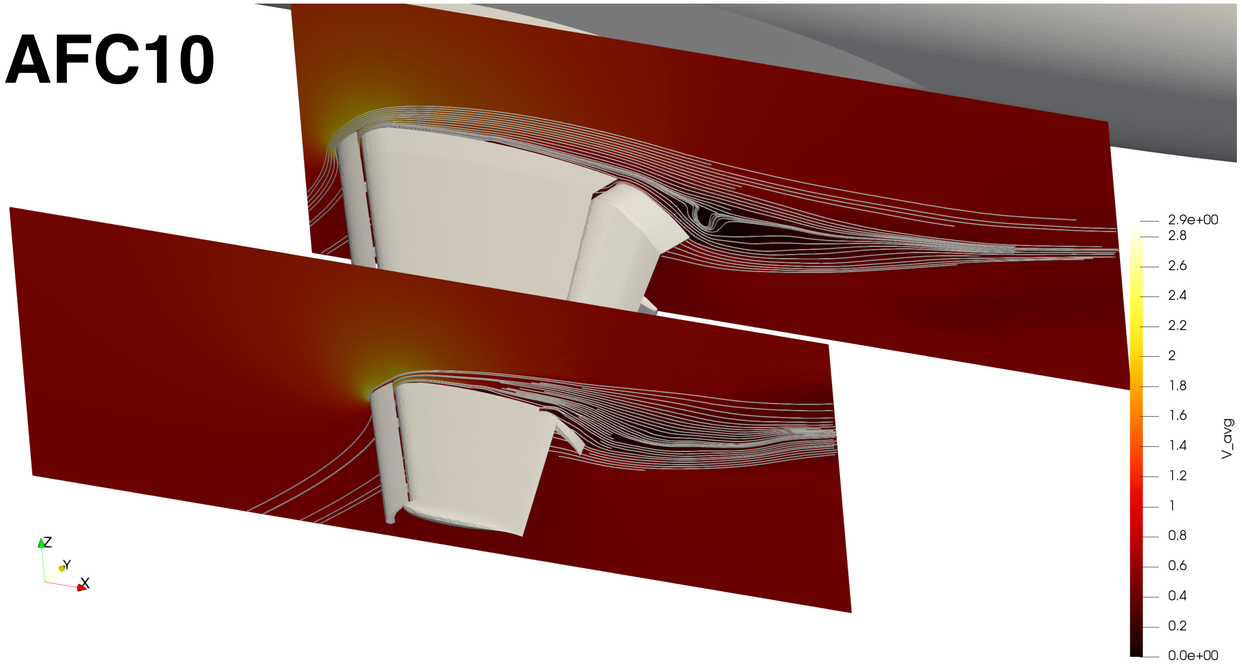
EXCELLERAT

JAXA High-lift AFC results: Maximum C_L

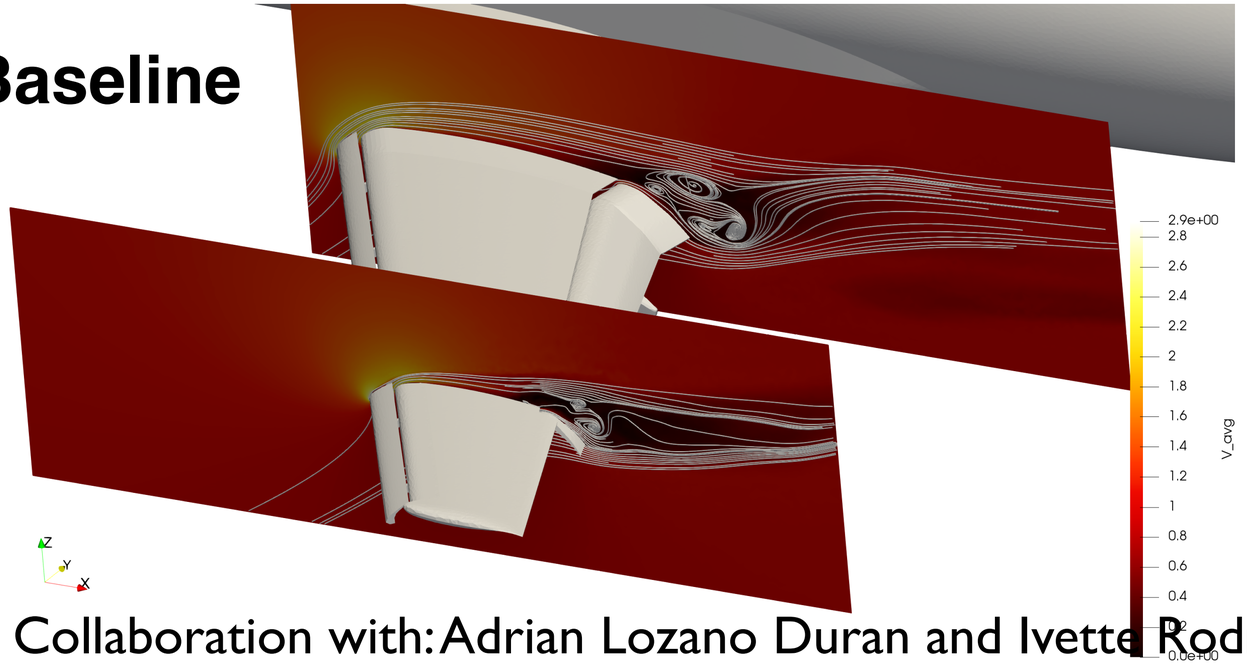


	C_L	C_D	C_L/C_D
Baseline	2.685	0.405	6.630
AFC10	**2.754(2.6%)**	0.391 (3.5%)	7.040 (6.2%)

AFC10



Baseline

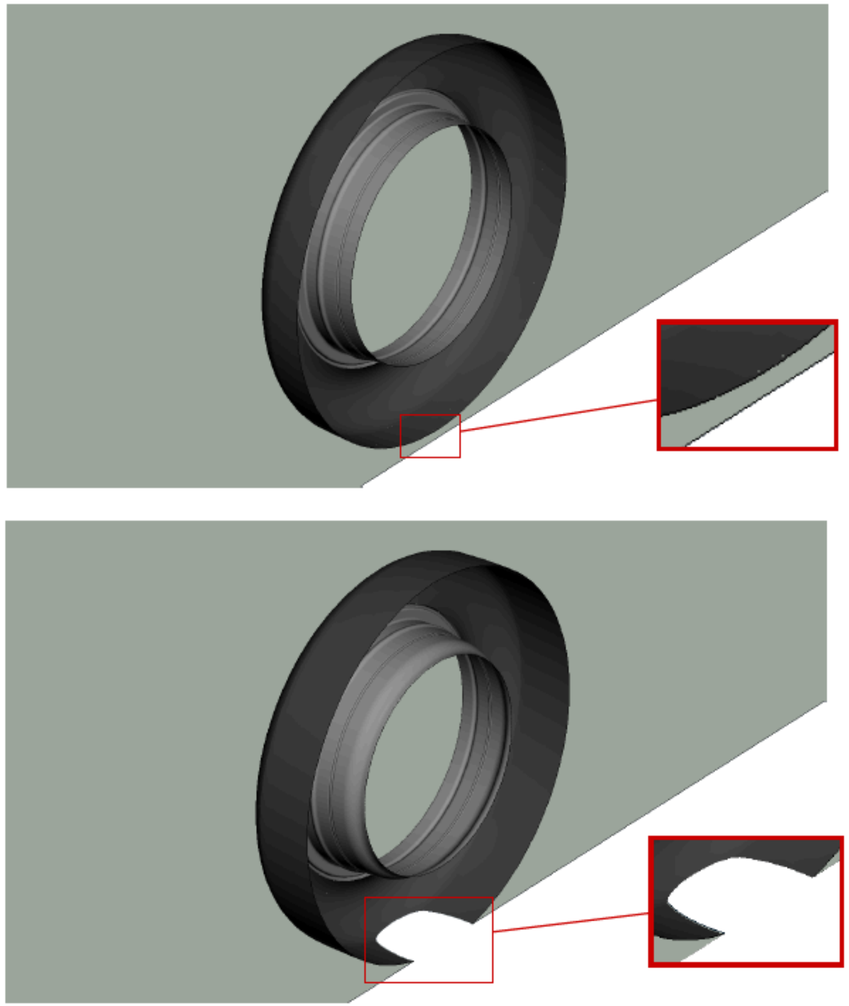


Collaboration with: Adrian Lozano Duran and Ivette Rodriguez

EXCELLERAT

wmLES of DrivAer at high Reynolds numbers

- DrivAer with wheel and ground interaction at Re = 4-8 M
- Meshes from 80M to 160 M of elements
- Vreman SGS model used with equilibrium wall model



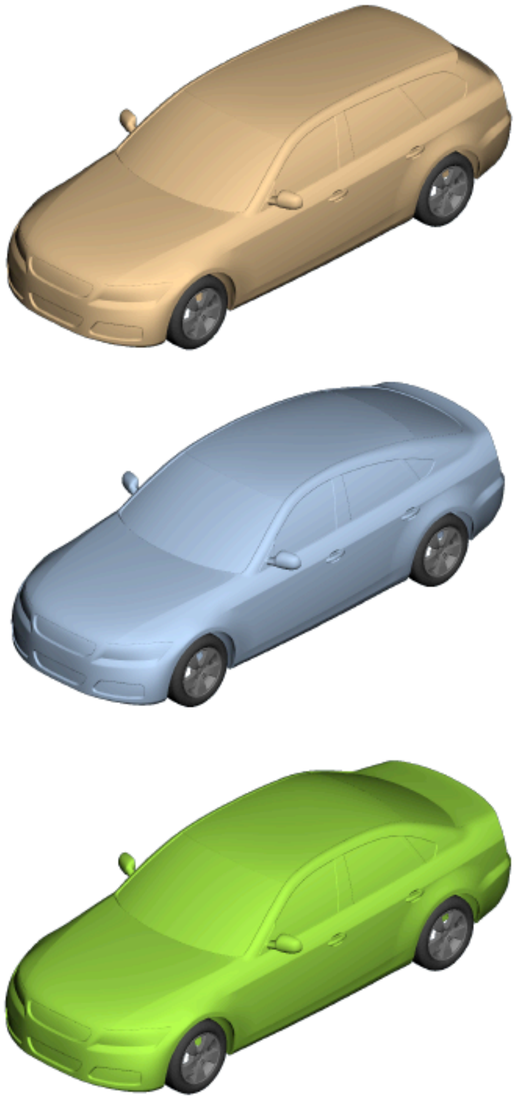


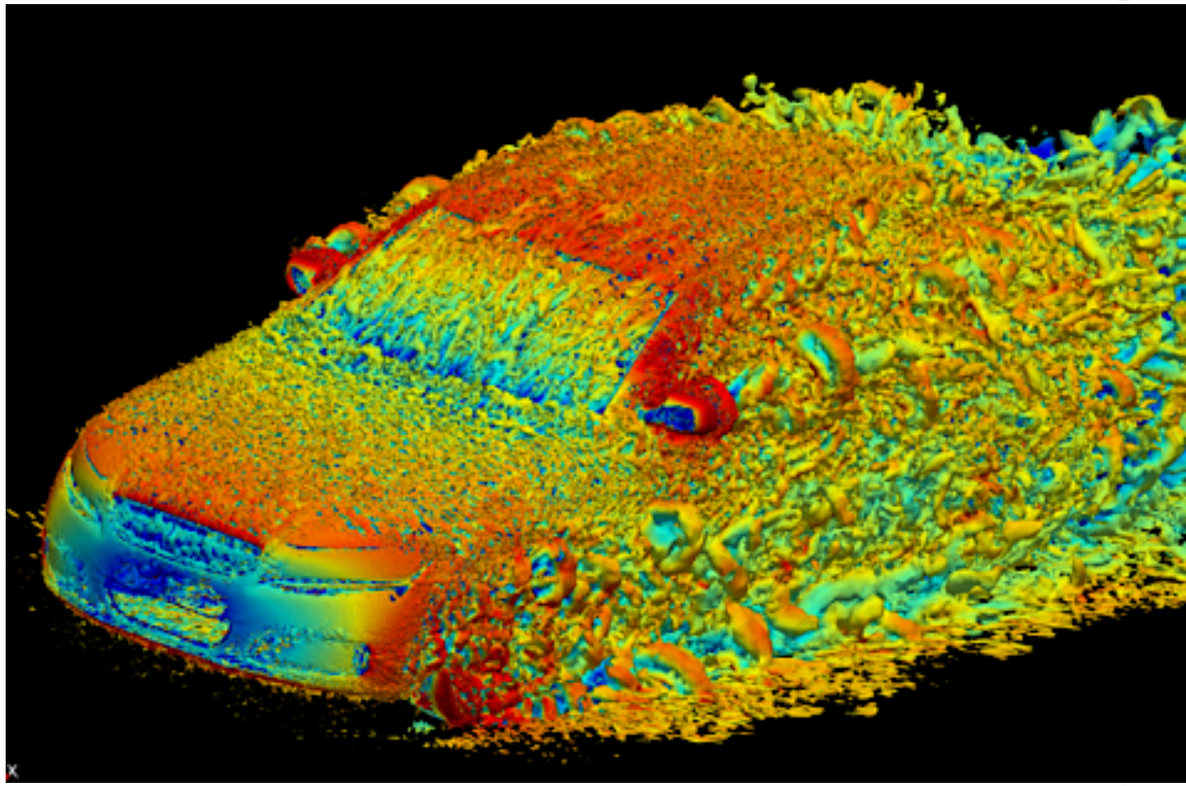
Figure 6: DrivAer geometries. Top) estateback ; middle) fastback ; bottom) notchback.

Barcelona Supercomputing Center

wmLES of DrivAer at high Reynolds numbers

Table 1: Drivaer with ground simulation ($Re = 4.87 \times 10^6$). Aerodynamic force coefficient. Drag coefficient, C_D and lift coefficient, C_L, respectively.

		C_D	C_L
Fastback	slip	0.252	-0.040
	no-slip	0.259	-0.063
	experiment [26]	0.258	-0.060
Estateback	slip	0.334	0.104
	no-slip	0.316	-0.201
	experiment [26]	0.314	-0.200
Notchback	slip	0.268	-0.063
	no-slip	0.258	-0.058
	experiment [26]	0.270	-0.080



Barcelo enter

wmLES of DrivAer at high Reynolds numbers

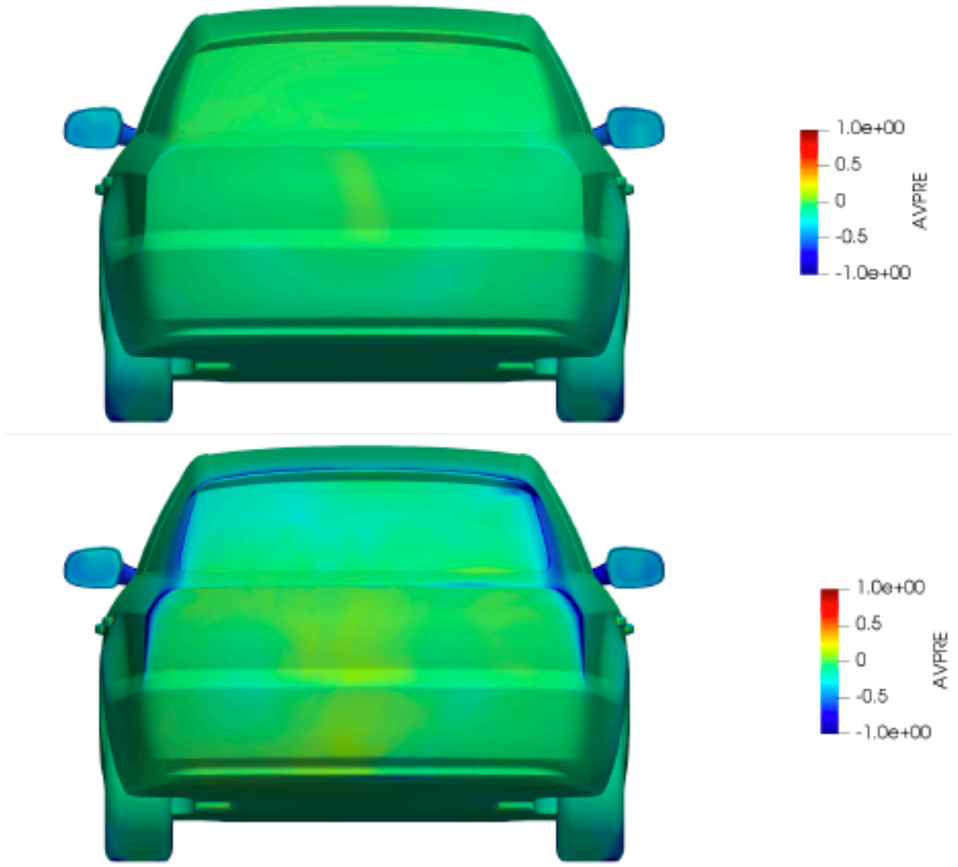


Figure 8: DrivAer estateback with ground simulation ($Re = 4.87 \times 10^6$). Averaged non-dimensional pressure at the car surface. Top) viscosity based non-slip wall model; bottom) slip wall model.

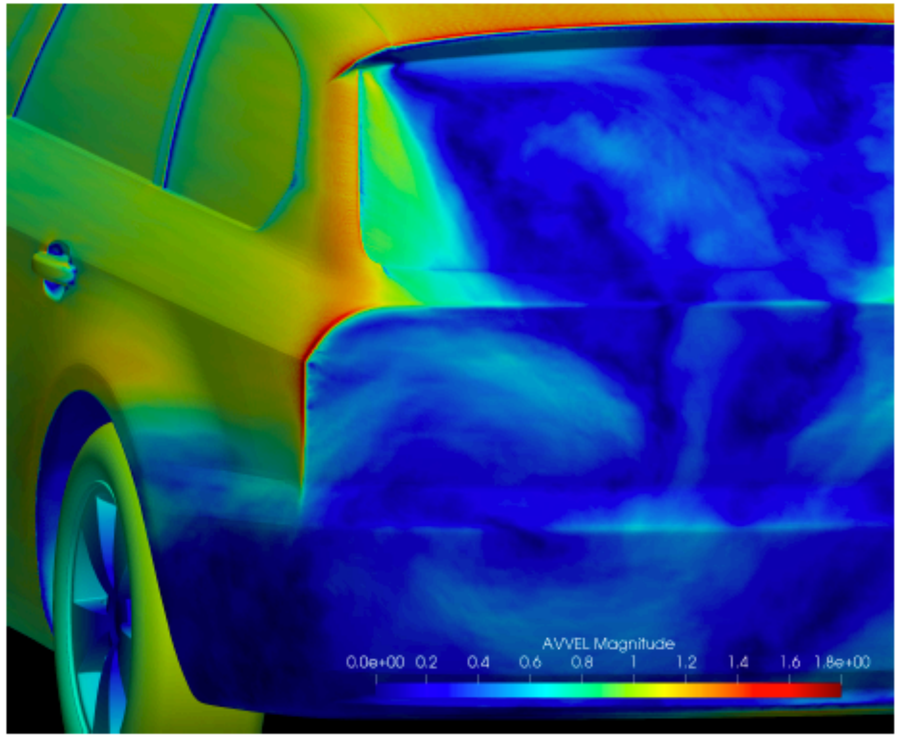
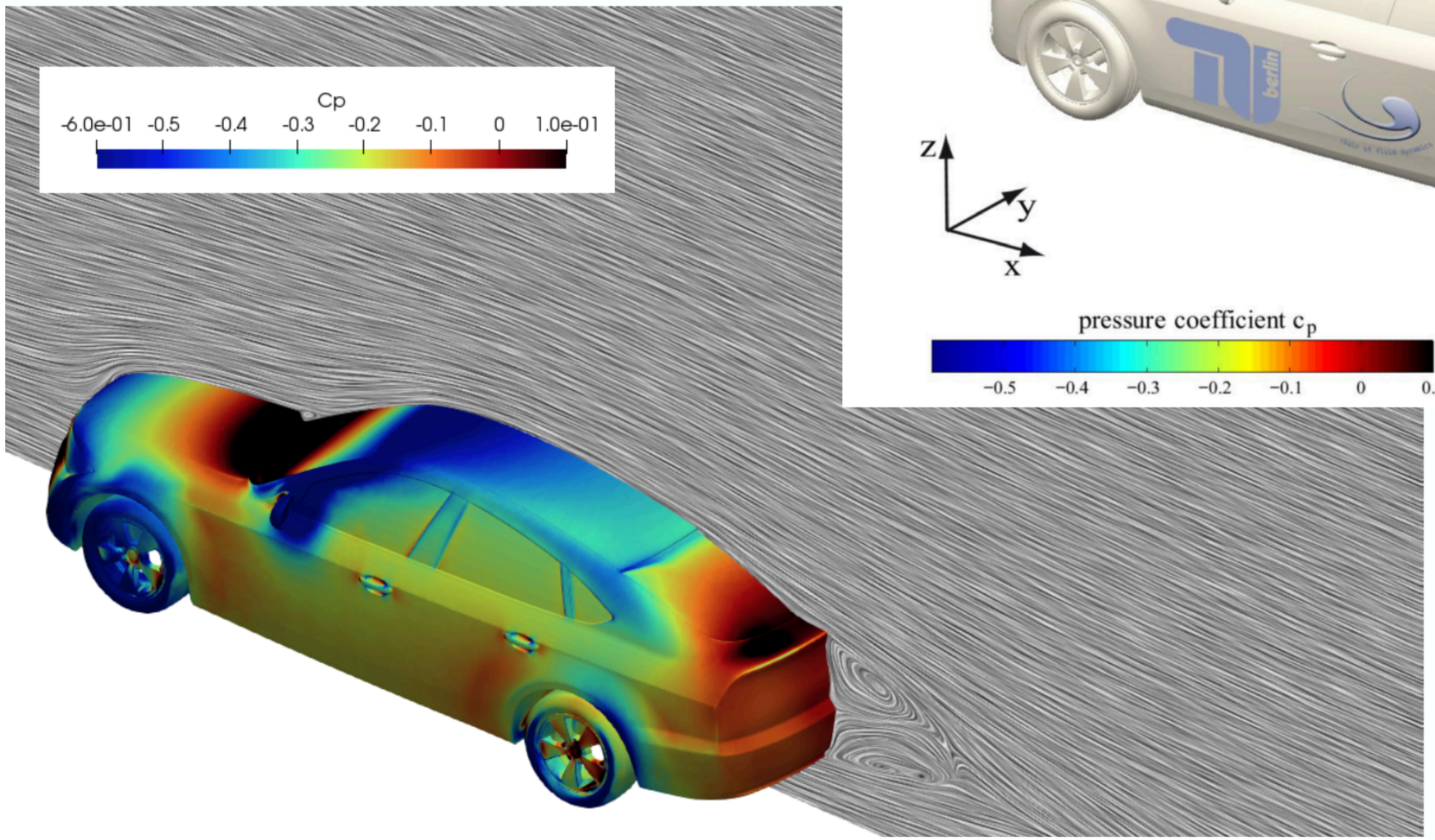
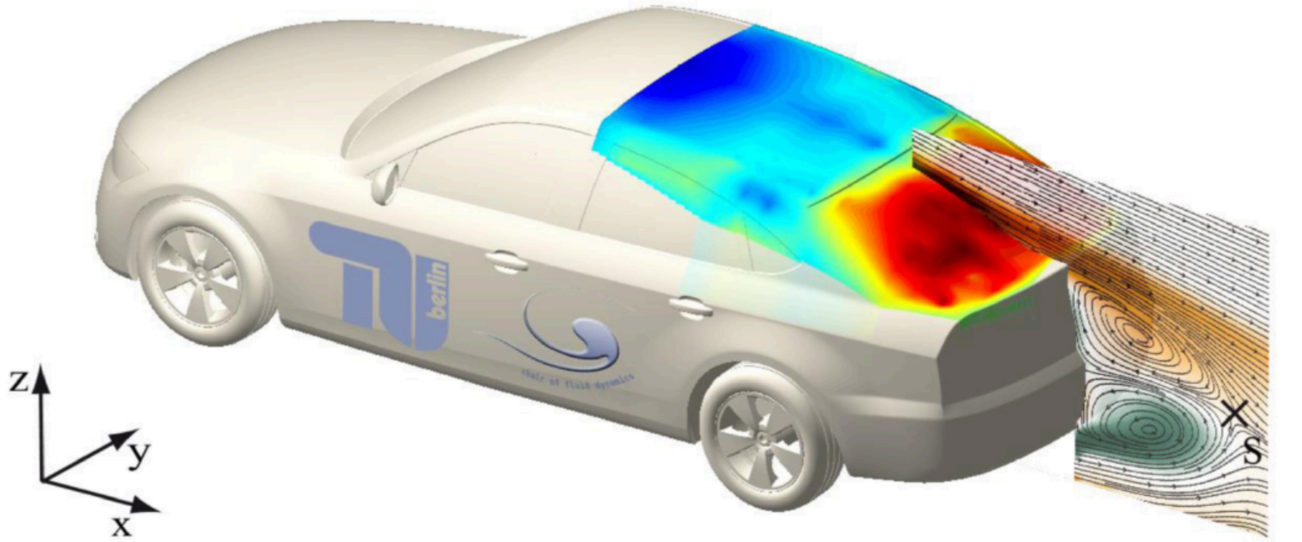


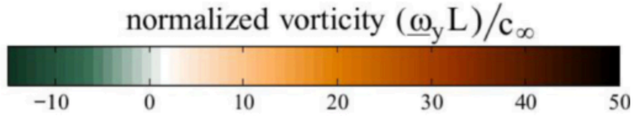
Figure 9: DrivAer estateback with ground simulation ($Re = 4.87 \times 10^6$) with slip wall model. Detail of the averaged non-dimensional slip wall velocity at the back of the car.

Barcelona Supercomputing Center

wmLES of DrivAer at high Reynolds numbers



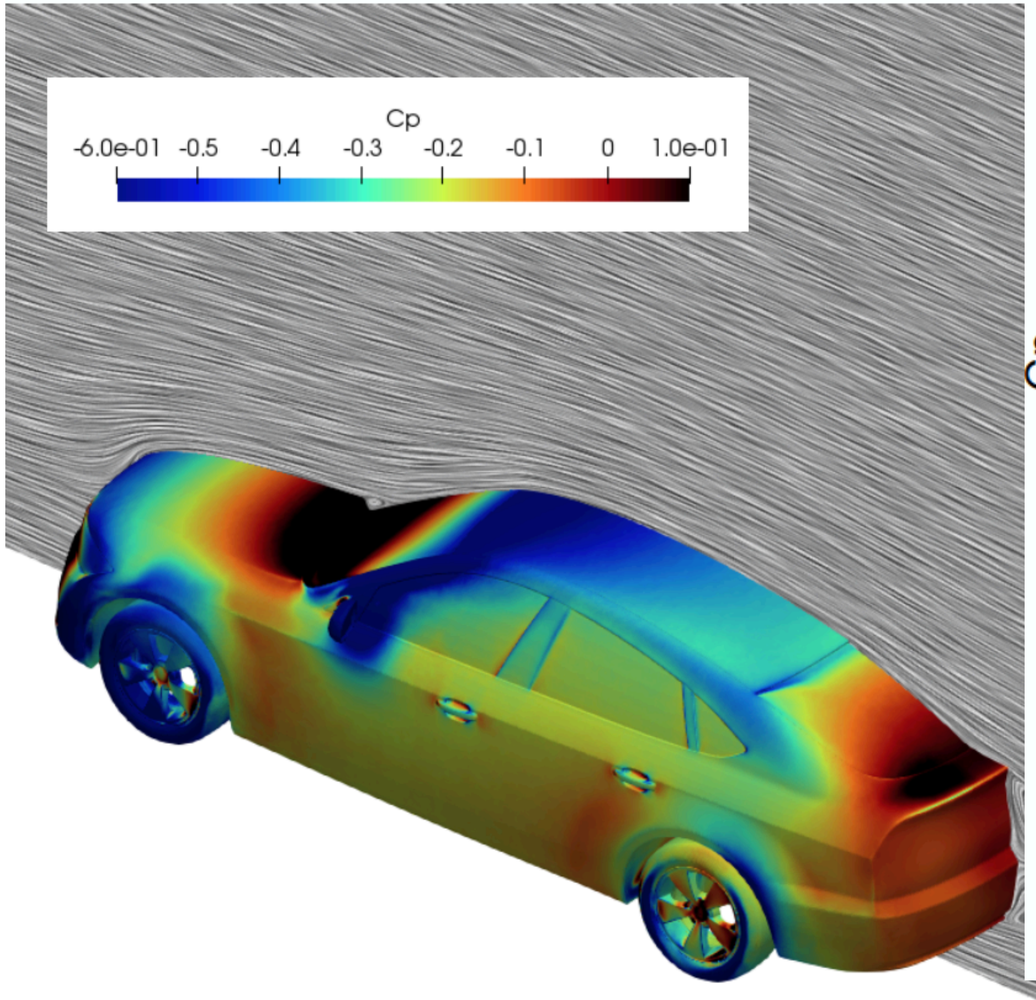


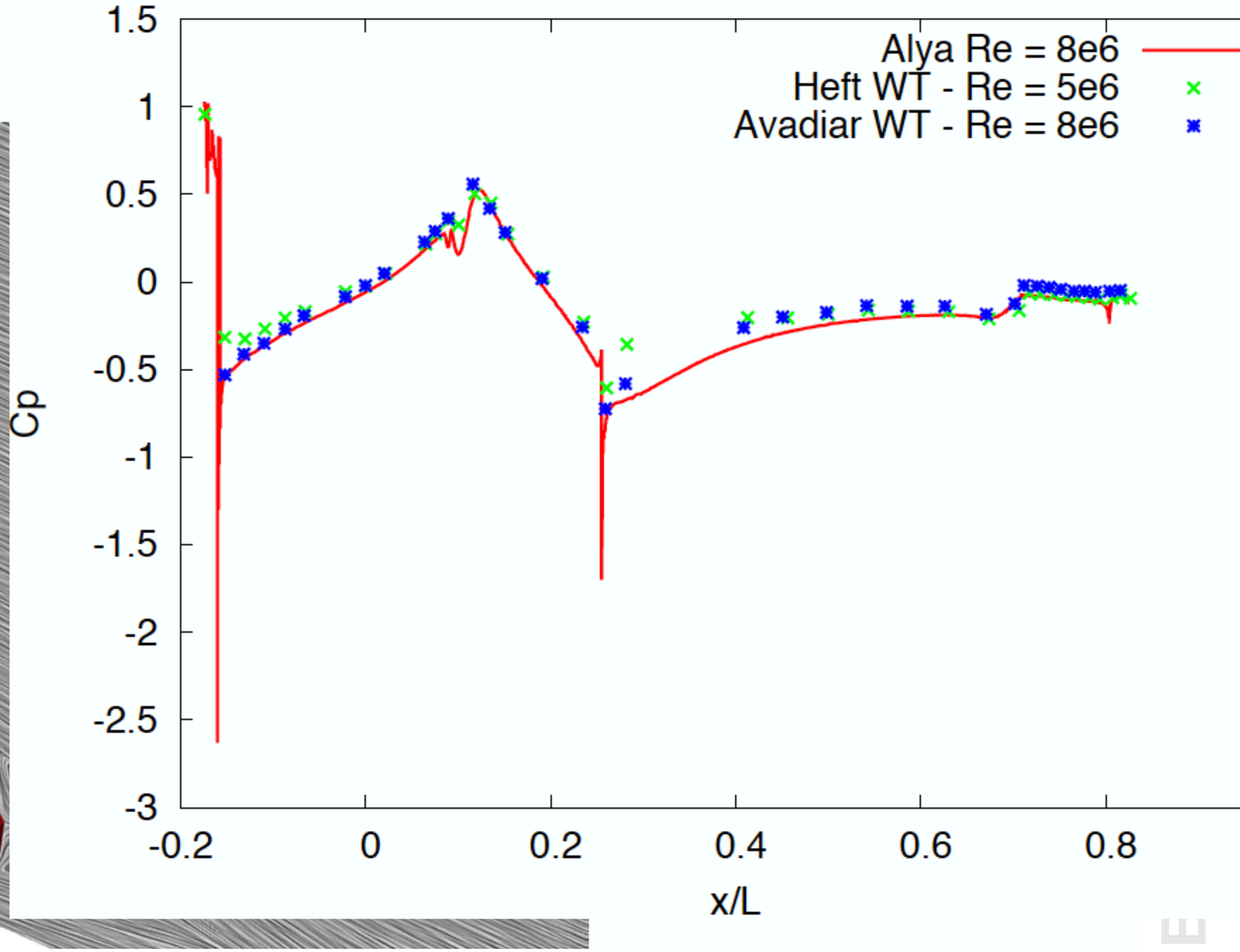


Experimental Study of Baseline Flow Characteristics for the Realistic Car Model DrivAer, Christoph Strangfeld et al. SAE 2013 World Congress and Exhibition

Barcelona Supercomputing Center

wmLES of DrivAer at high Reynolds numbers

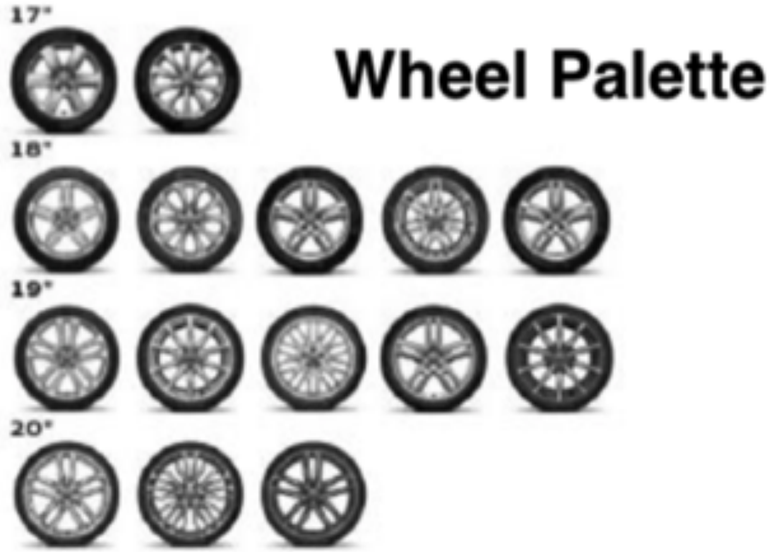


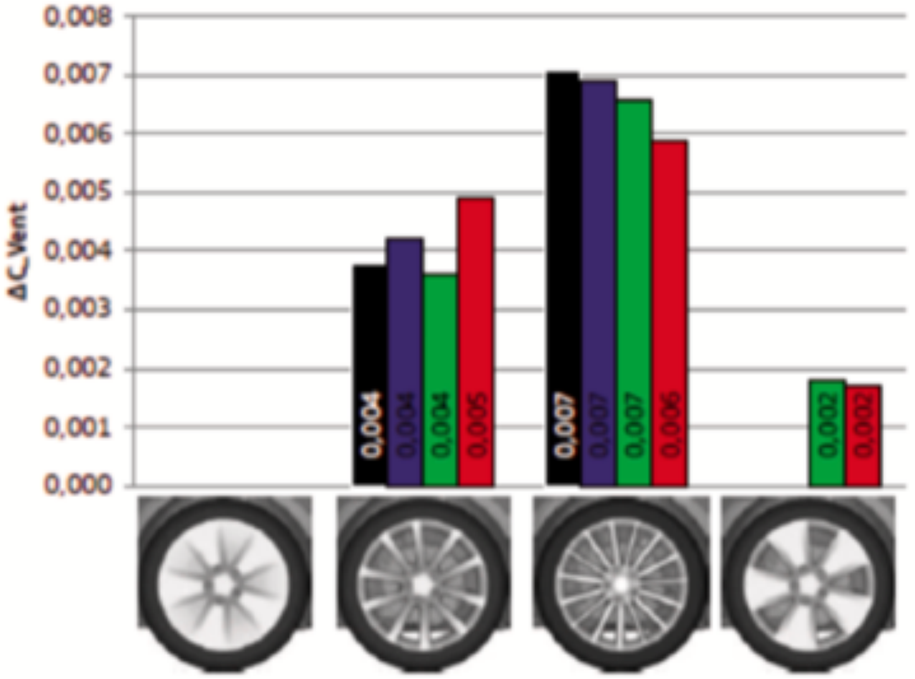


Can we go to real industrial conditions??

Motivation:

Two different factors are drivers for the current research proposal. First, 25% of the drag comes from the wheels, therefore it is believed to be a big optimization potential directly related to the wheel hub geometry. In this sense, more flow physics insight it is needed in order to understand the main physical mechanisms and how the wheel hub geometry impact over the overall flow topology. Secondly, given the current European legislation the drag influence of all wheels must be evaluated and declared. Hence, it is needed to develop an efficient CFD methodology to carry out this type of assessment accurately.





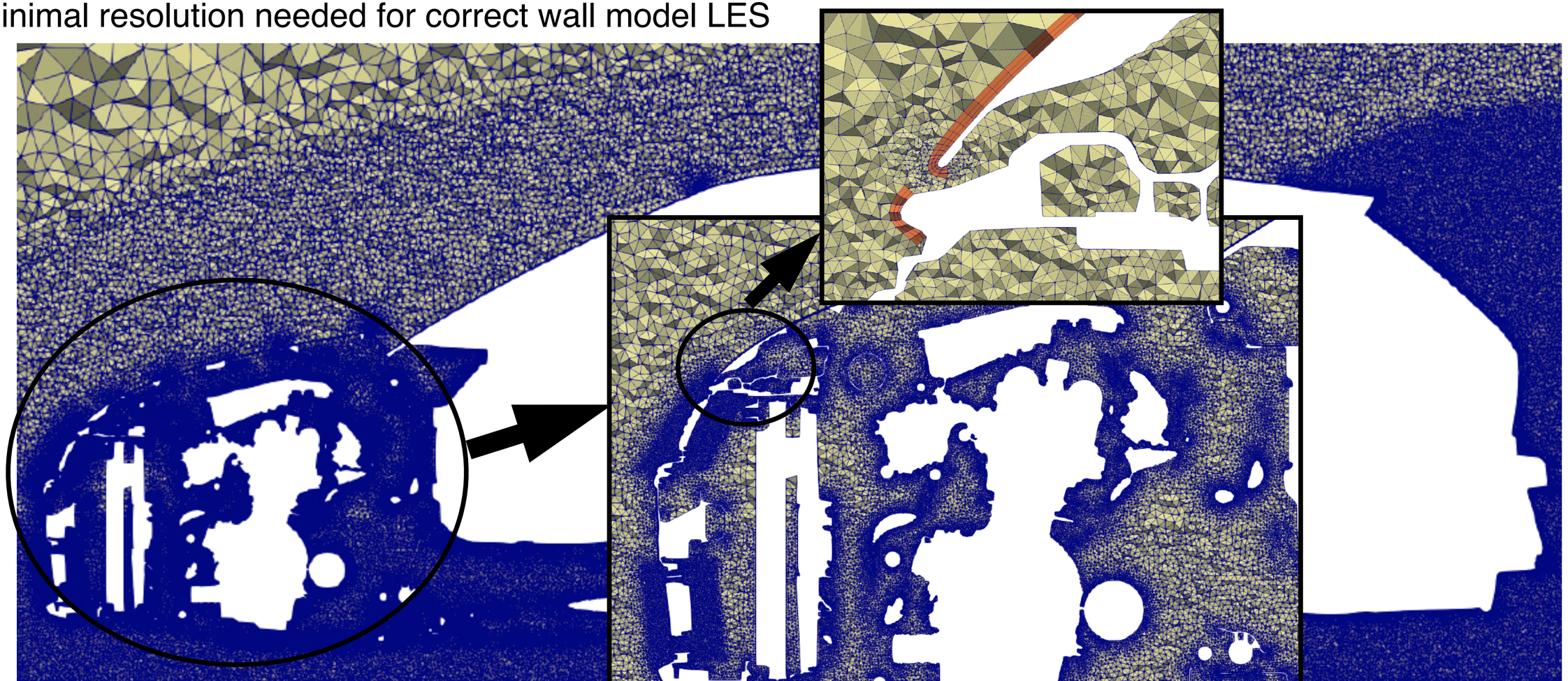
SEAT

Barcelona Supercomputing Center

Can we go to real industrial conditions??: the mesh issue

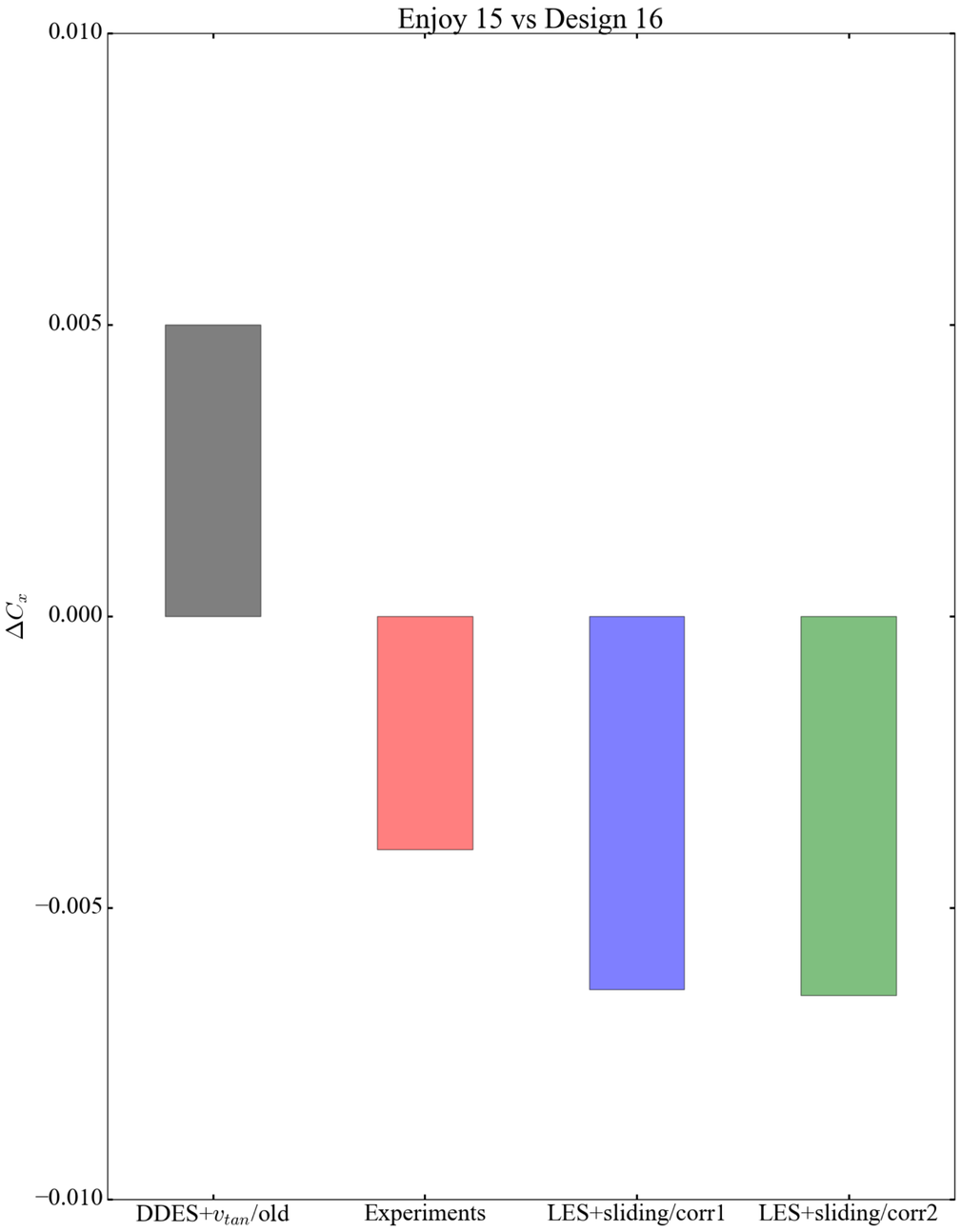
Adaptation of the geometry and generation of meshes optimal for LES

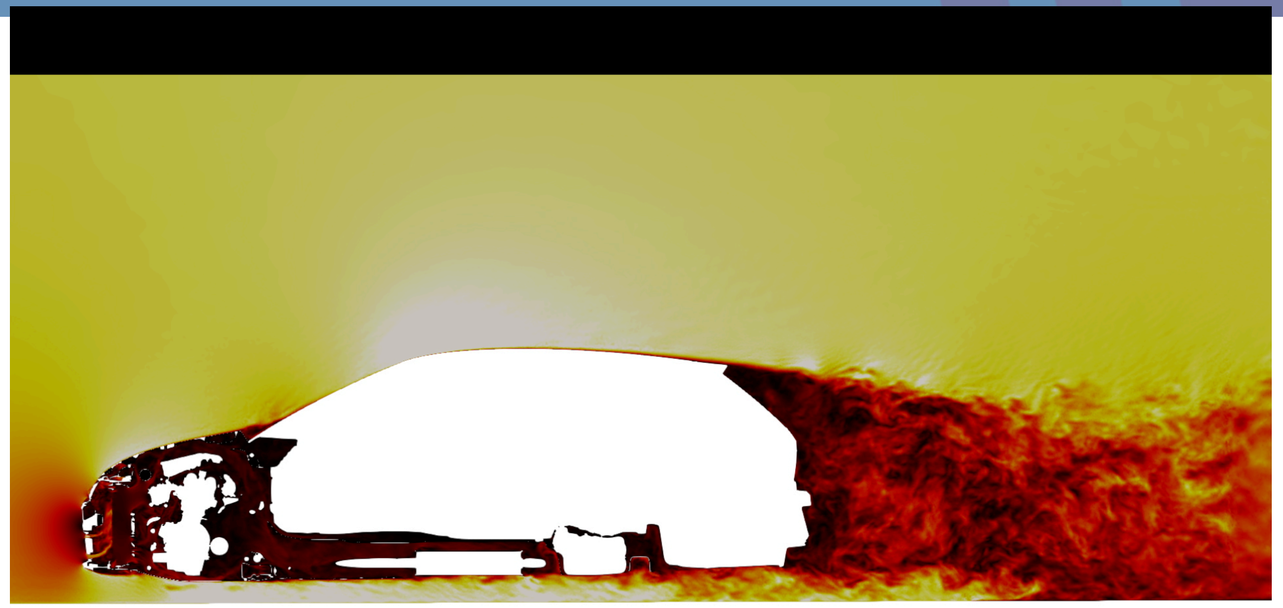
- ANSA mesh tool used to build LES compatible meshes, full wind tunnel modelled.
- Extensive work in order to have a water tight like geometry
- Meshes of 300-500M elements with 3-10 elements in the BL generated
- Is the minimal resolution needed for correct wall model LES

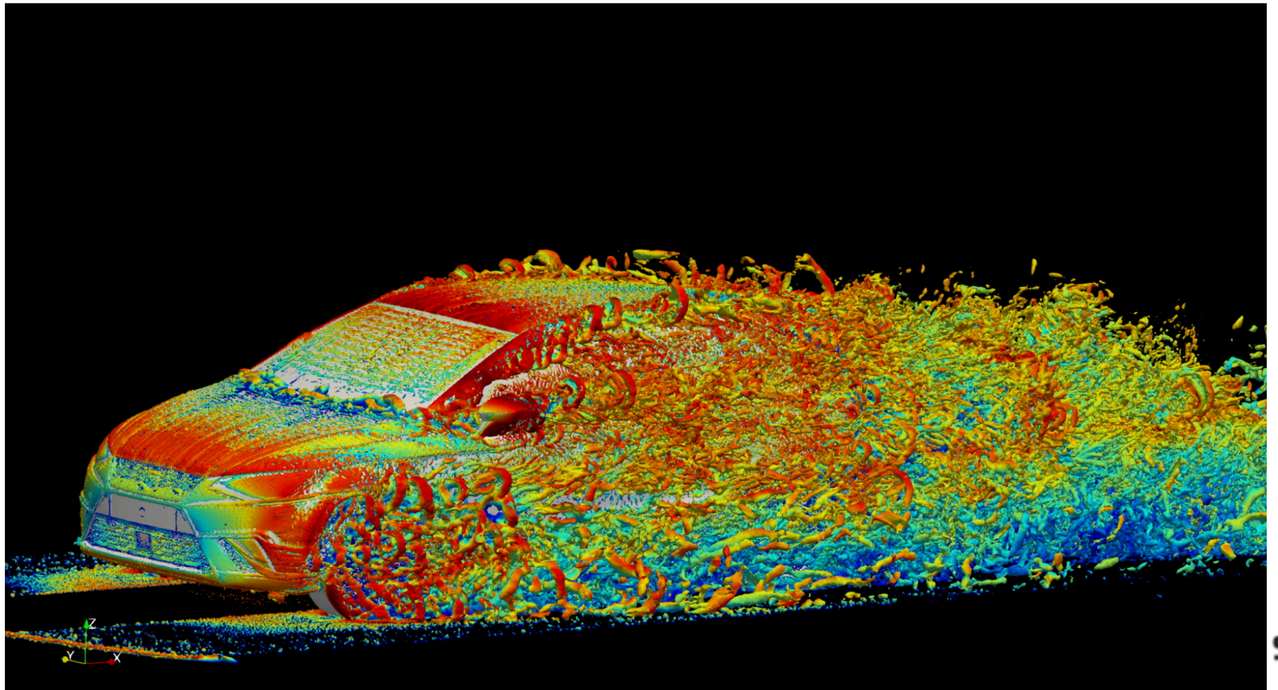


Barcelona Supercomputing C r

Can we go to real industrial conditions??: some results





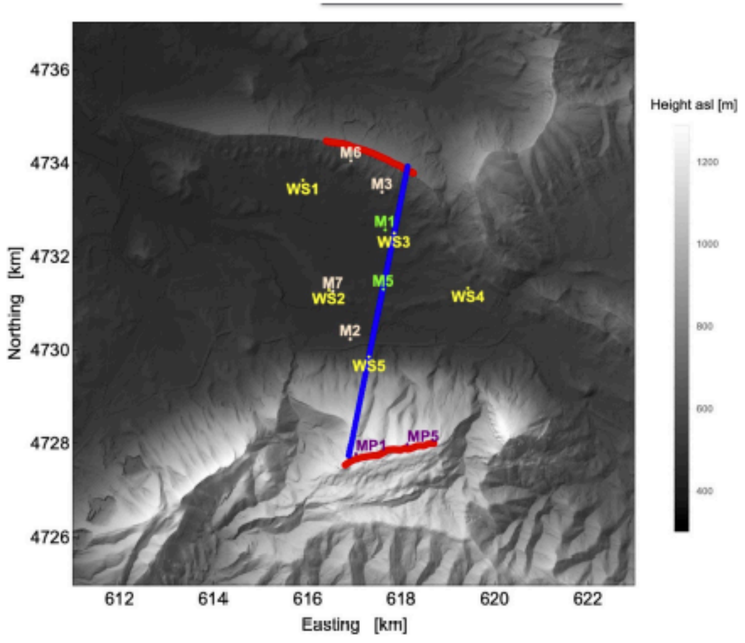


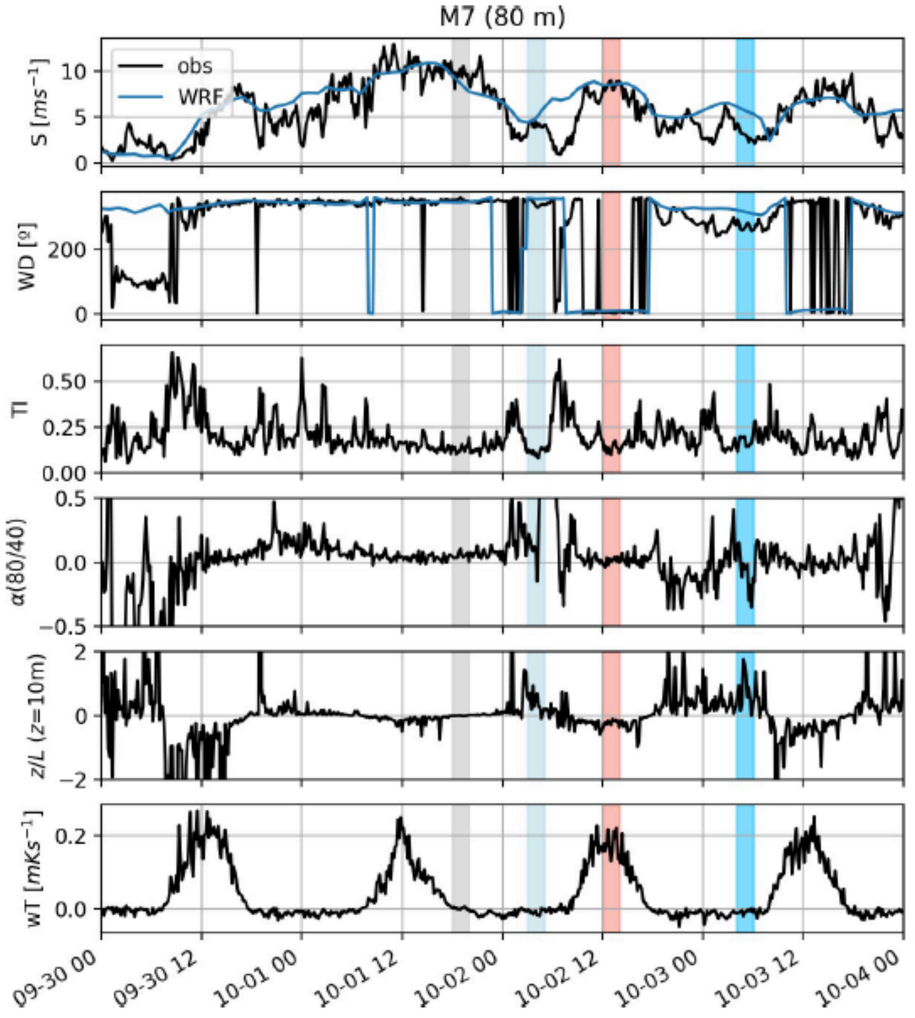
rcelona Supercomputing Center

SEAT

The ALEX 17 exercise (IEA Task 31)

- The NEWA ALEX17 experiment was conducted with the objective of characterizing the wind conditions upstream of the Alaiz Test Site for the validation of flow models.
- Data for meso-micro scale coupling is given in the benchmark.
- Several groups trying different coupling techniques are participating.
- A great learning experience for the ENERXICO developments!
- A paper lead by J. Sanz has been submitted with extensive validations.





arcelona Supercomputing Center
ERDROLA

Wind energy resource assessment

SCM with Large-Scale Tendencies and Data Assimilation

- Mesoscale forcing
- Solved at microscale
- Data assimilation at microscale

$$\frac{1}{f_c}\frac{\partial U}{\partial t} = U_{adv} + V + U_{pg} - \frac{1}{f_c}\frac{\partial \overline{uw}}{\partial z} + U_{nud}$$

$$\frac{1}{f_c}\frac{\partial V}{\partial t} = V_{adv} - U + V_{pg} - \frac{1}{f_c}\frac{\partial \overline{vw}}{\partial z} + V_{nud}$$

$$\frac{\partial \Theta}{\partial t} = \Theta_{adv} - \frac{\partial \overline{w\theta}}{\partial z} + \Theta_{nud}$$

- No humidity
- No heat transfer by radiation or phase changes

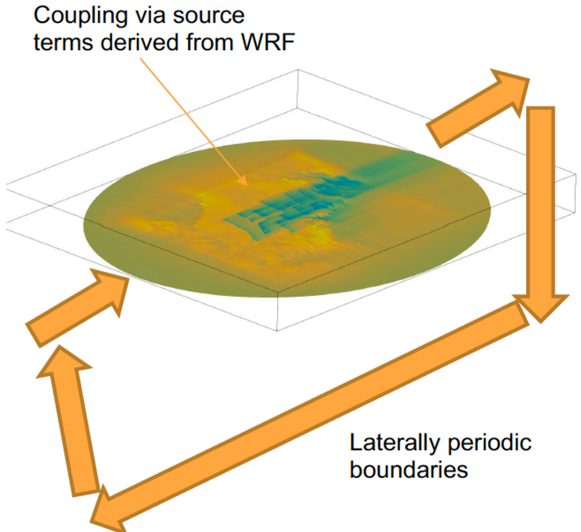
$$\delta_{nud} = \frac{\omega_z}{f_c}\frac{\left(\delta_{obs} - \delta\right)}{\tau_{nud}}$$

$\tau_{nud} = 10\text{min} : 1\text{hr}$

$\omega = 1$ within measurements

- M-O at the surface based on mesoscale inputs

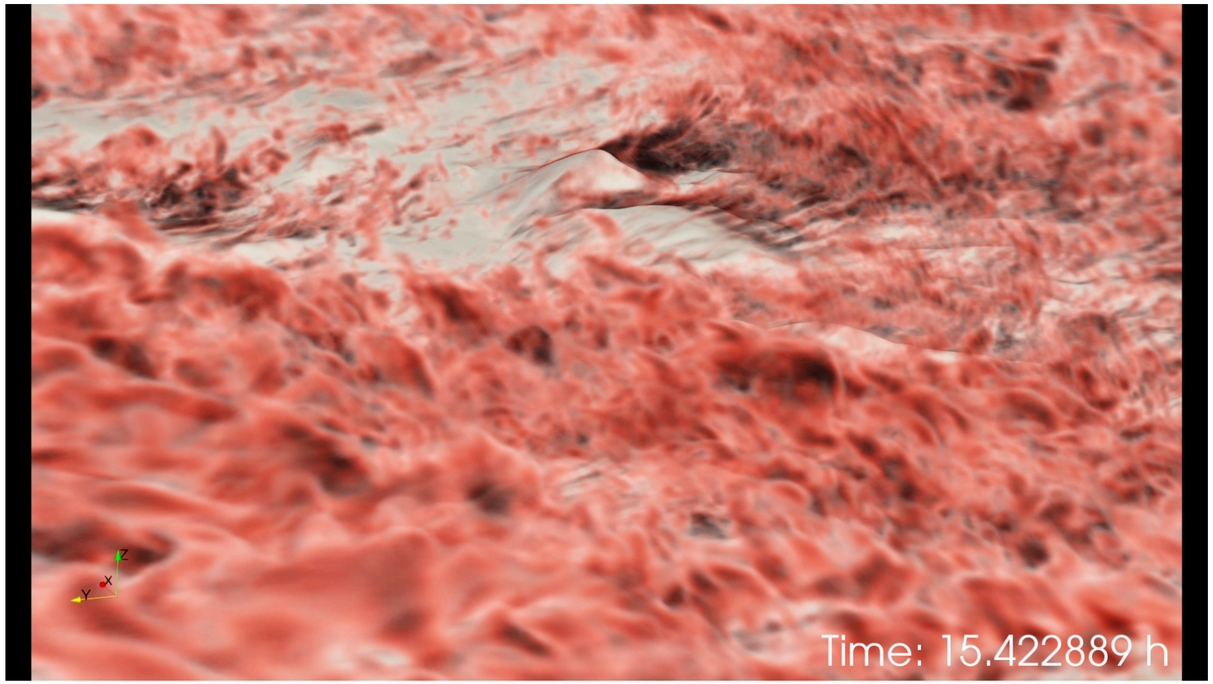
$$\Theta_2 = \Theta_0 + \frac{\theta^*}{\kappa}\left[\lg\left(\frac{2}{z_{0t}}\right) + \Psi_h\left(\frac{2}{L_0}\right)\right]; \quad \theta^* = -\frac{\overline{w'\theta'}}{u^*}$$

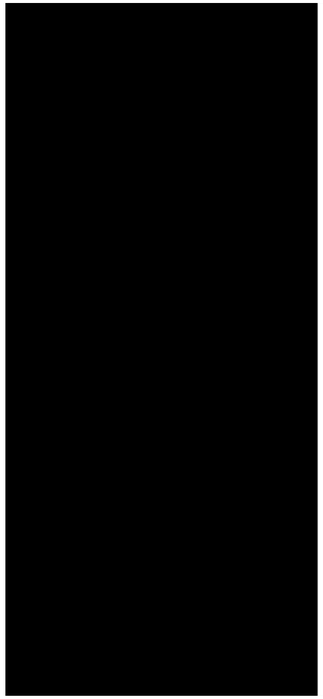


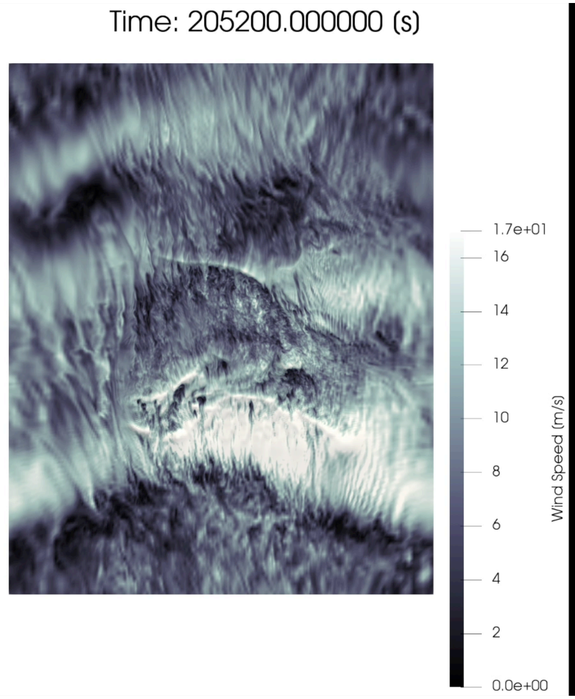
percomputing Center

Wind energy resource assessment

- Both LES and RANS solvers of Alya are coupled with forcing terms to WRF.
- The same forcing terms are used for both solvers, very similar mesh resolutions used, with some differences in the near wall mesh.
- For the RANS solver: k-epsilon closure of Sogachev et al., 16x15 km with tangential resolution of 50m.
- For the LES solver: Smagorinsky model with algebraic wall model, 16x15 km with tangential resolution of 35m.



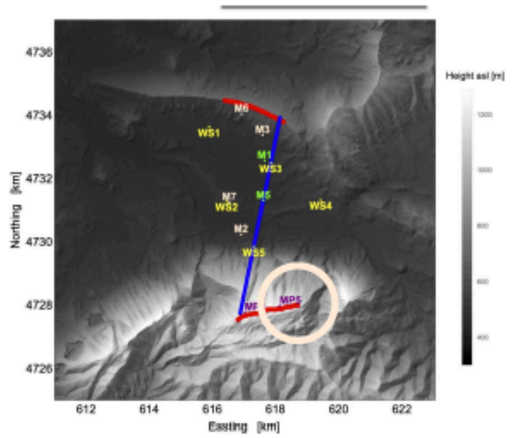


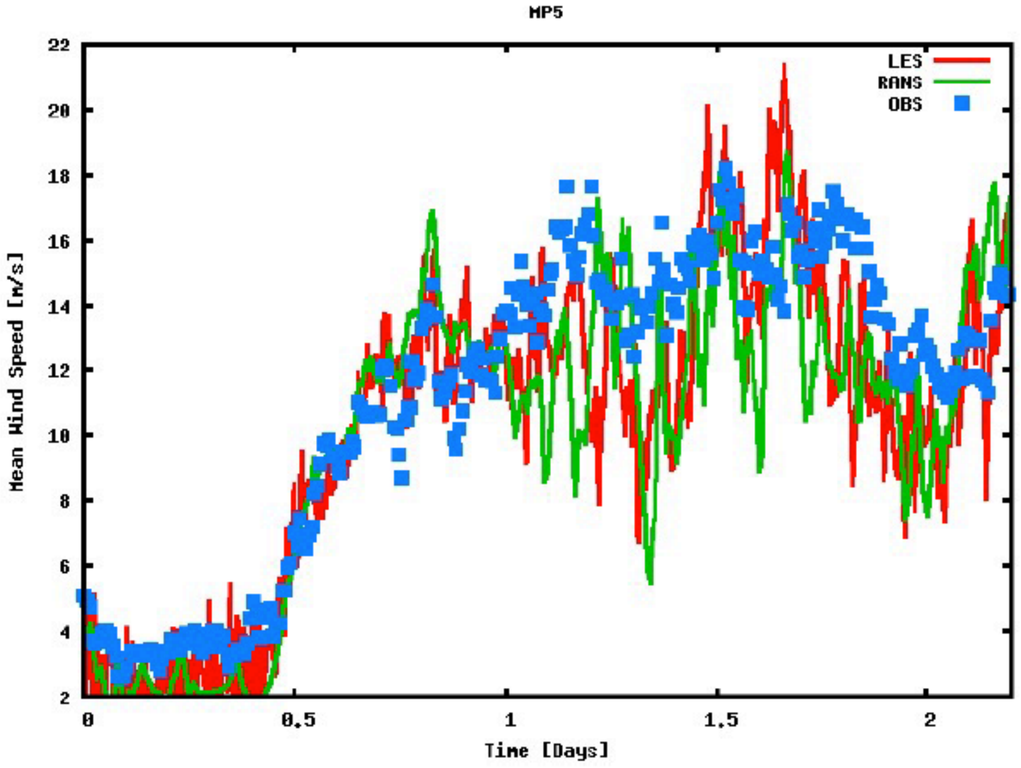


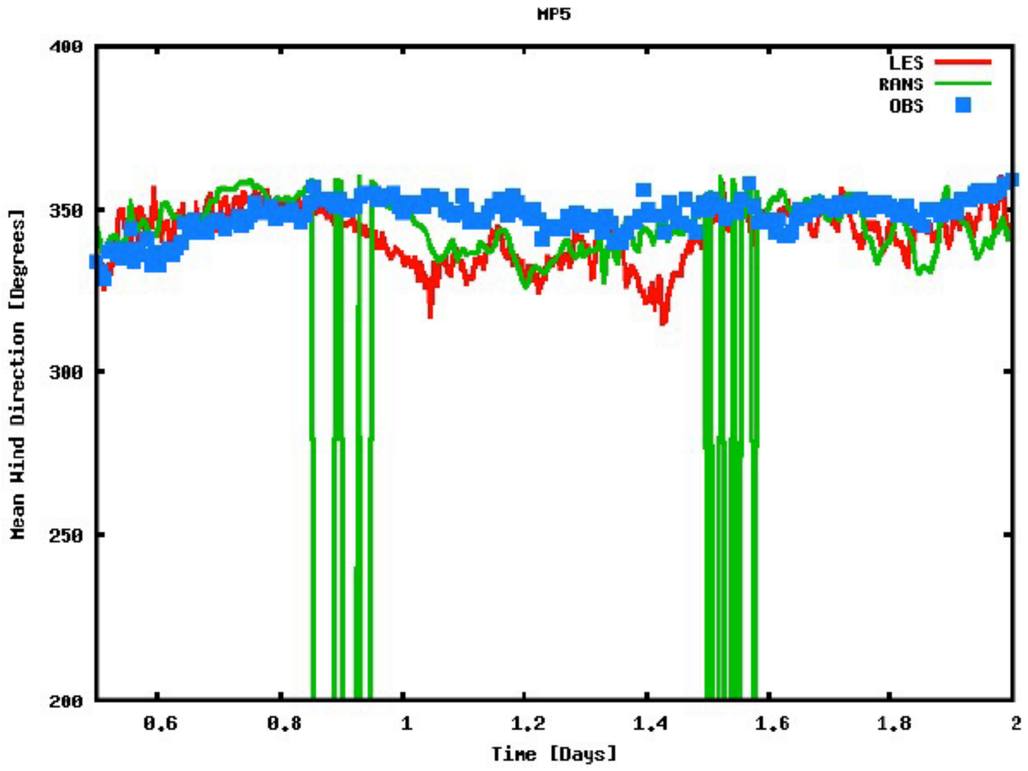
mputing Center

IBERDROLA

The ALEX 17 exercise (IEA Task 31)



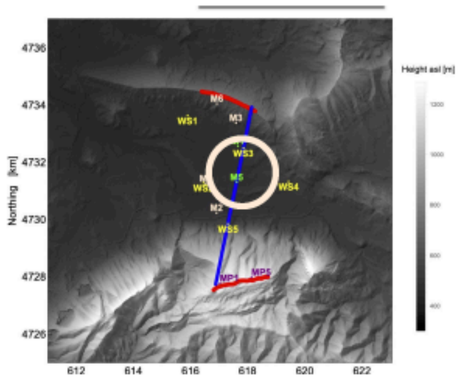


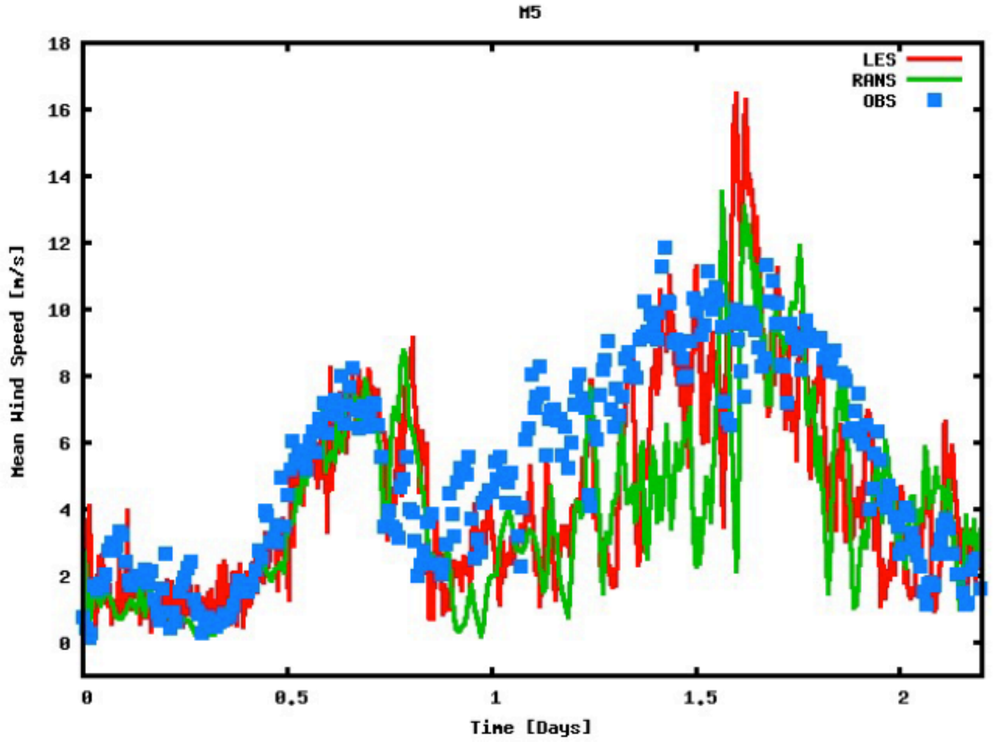


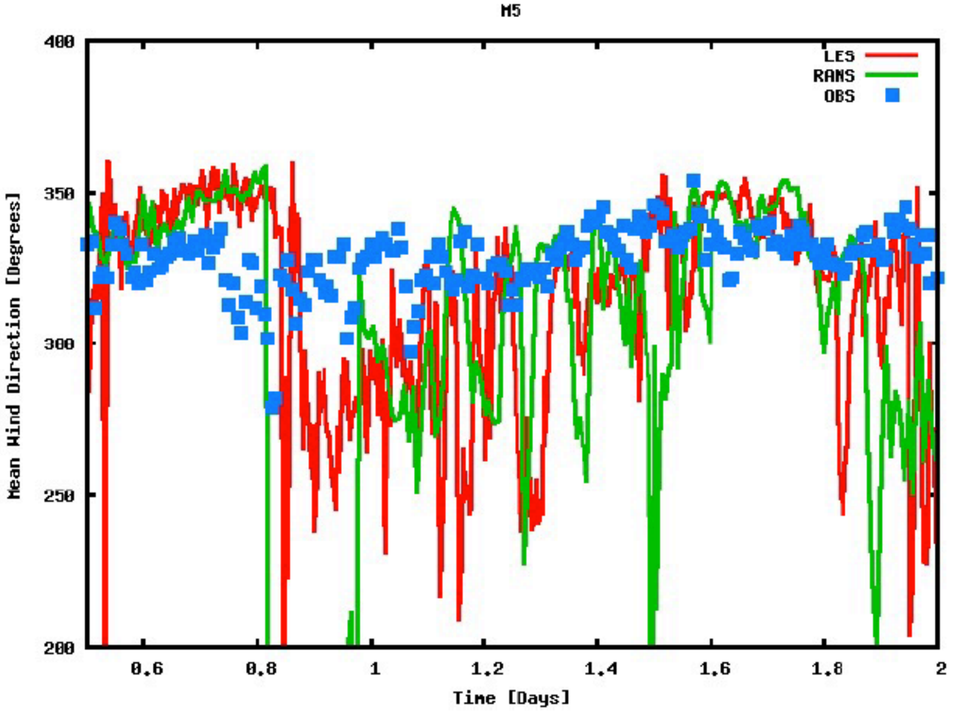
arcelona Supercomputing Center

IBERDROLA

The ALEX 17 exercise (IEA Task 31)





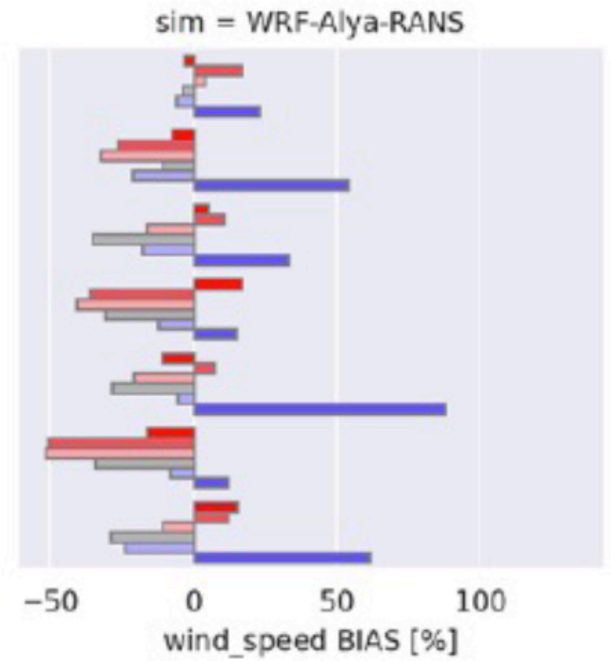


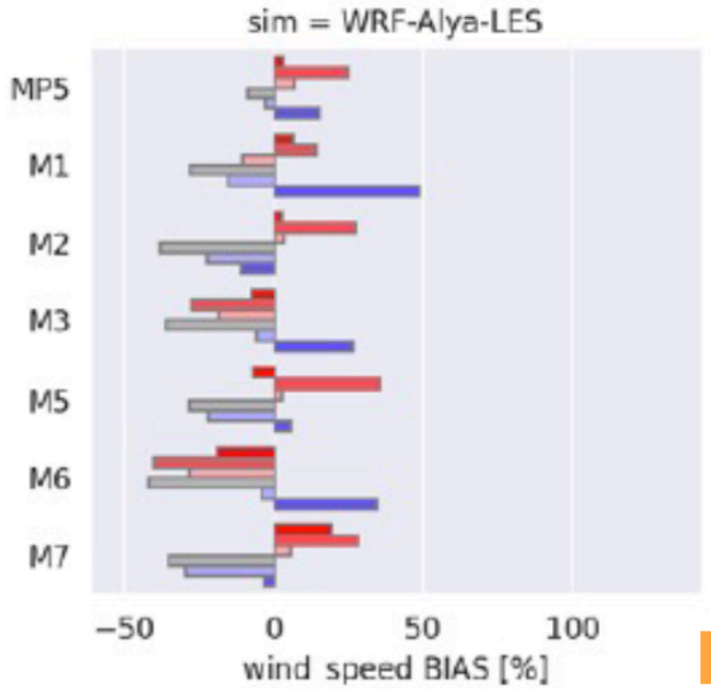
arcelona Supercomputing Center

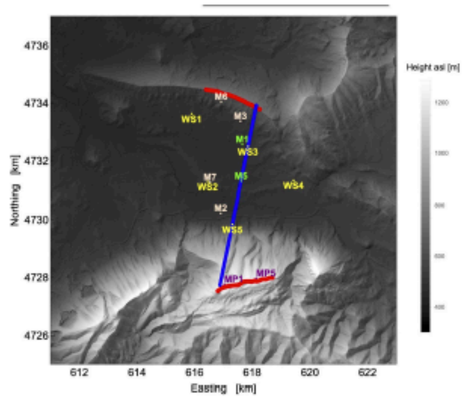
IBERDROLA

Wind energy resource assessment

The ALEX 17 exercise (IEA Task 31)









Model	Bias [%]
WRF (3km)	32.04
WRF+RANS	-4.23
WRF+LES	-3.74

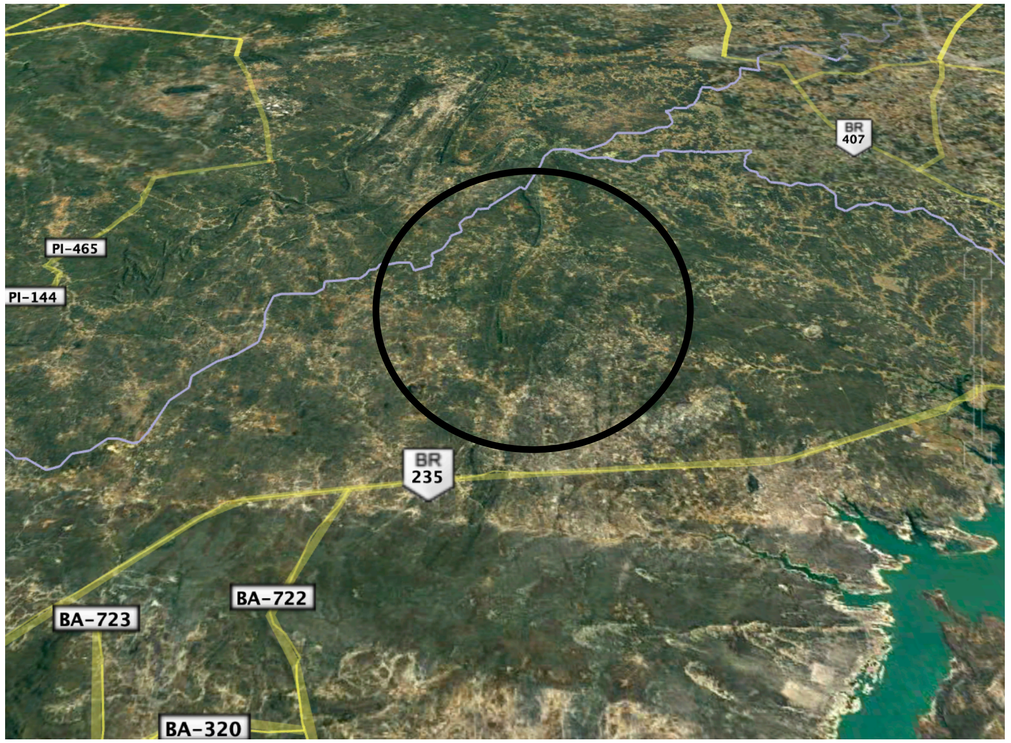
Internal Use

arcelona Supercomputing Center

IBERDROLA

Wind energy resource assessment

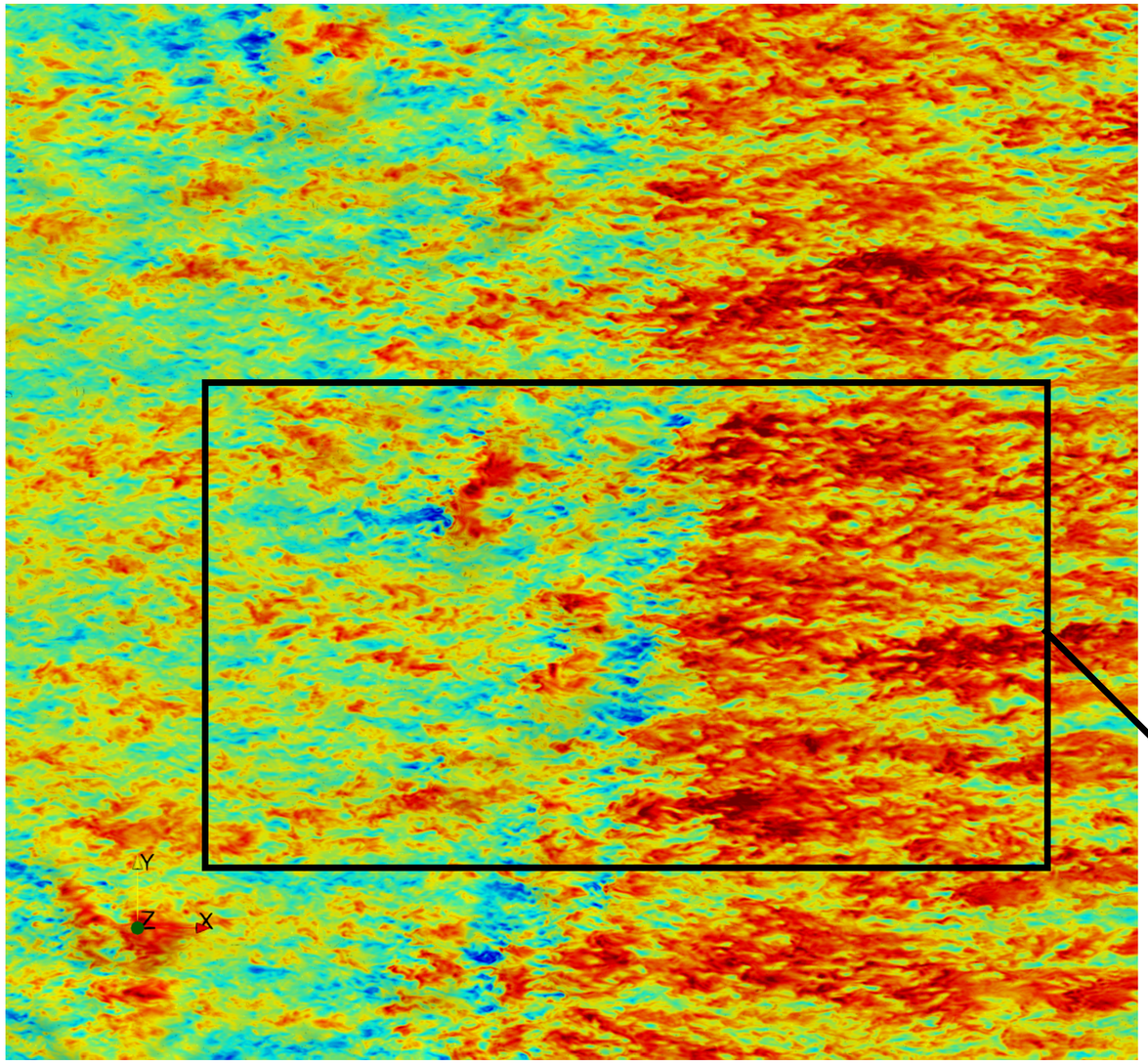
- A real wind farm from Iberdola tested
- The domain is : 12km x 12km x 2 km
- Two wind directions considered : E and ESE
- Meshes of O(100m) with a minimal resolution of 1 m





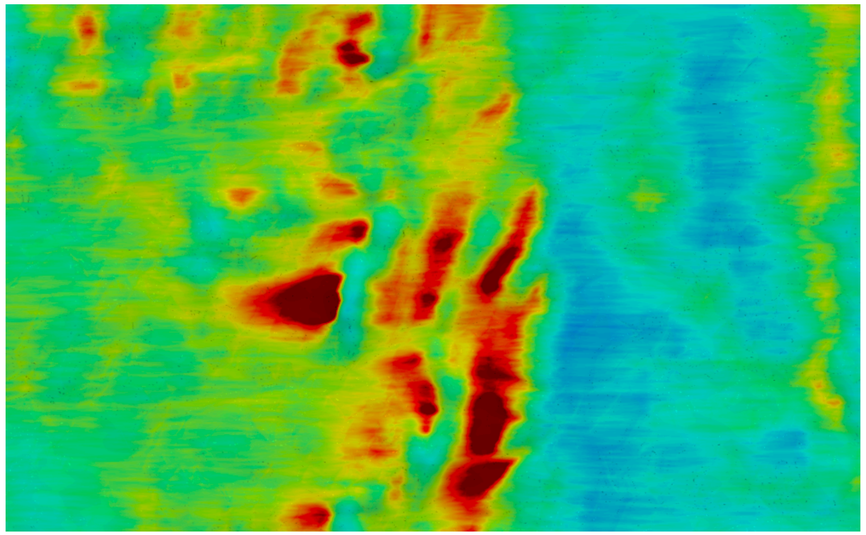
IBERDROLA

Wind energy resource assessment



Wind speed

- Just as example the E direction is shown
- There is a reduction of the wind speed du the effect of the mountains.
- Turbulence intensity is increased substantially because of the terrain impact.

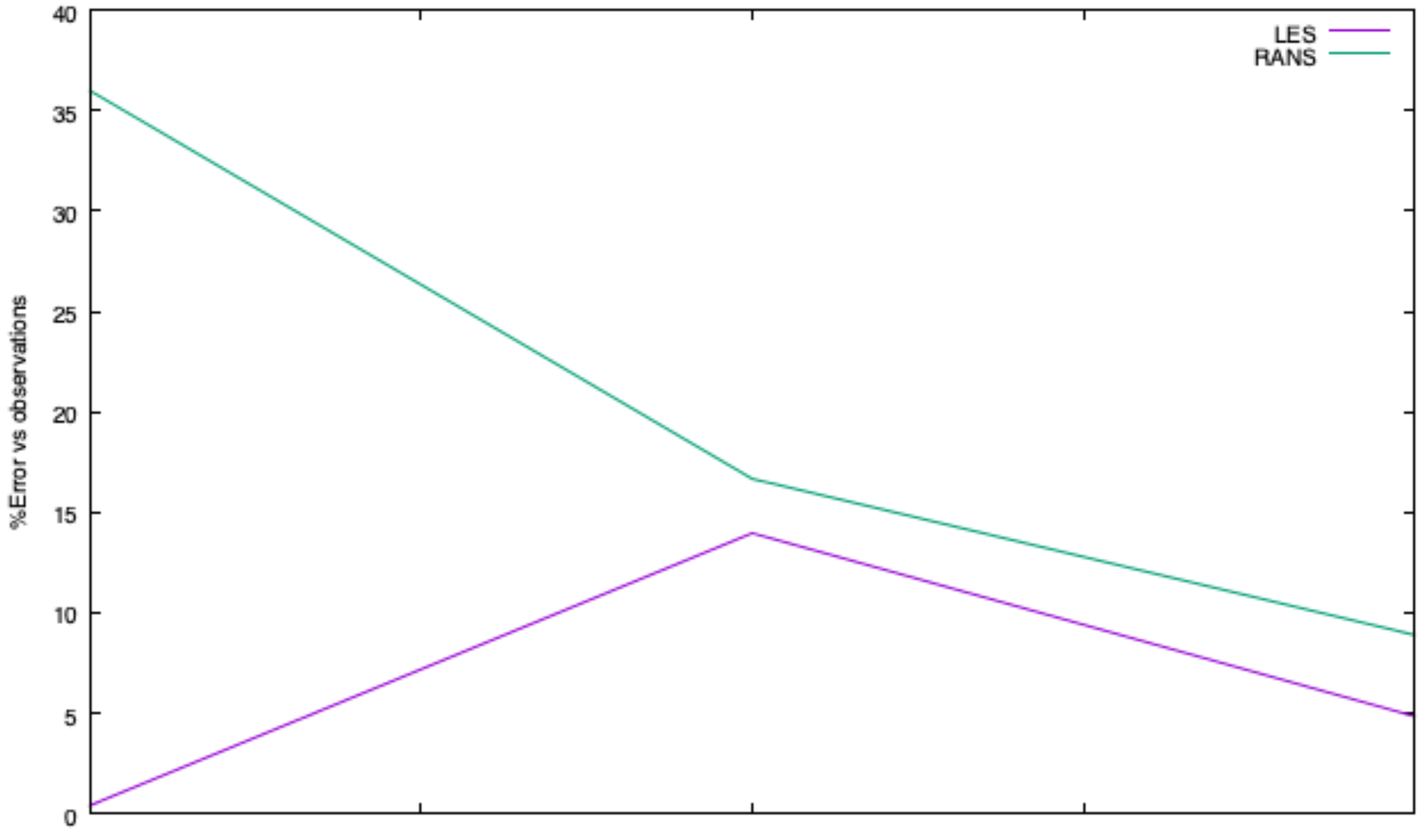


Turbulence Intensity

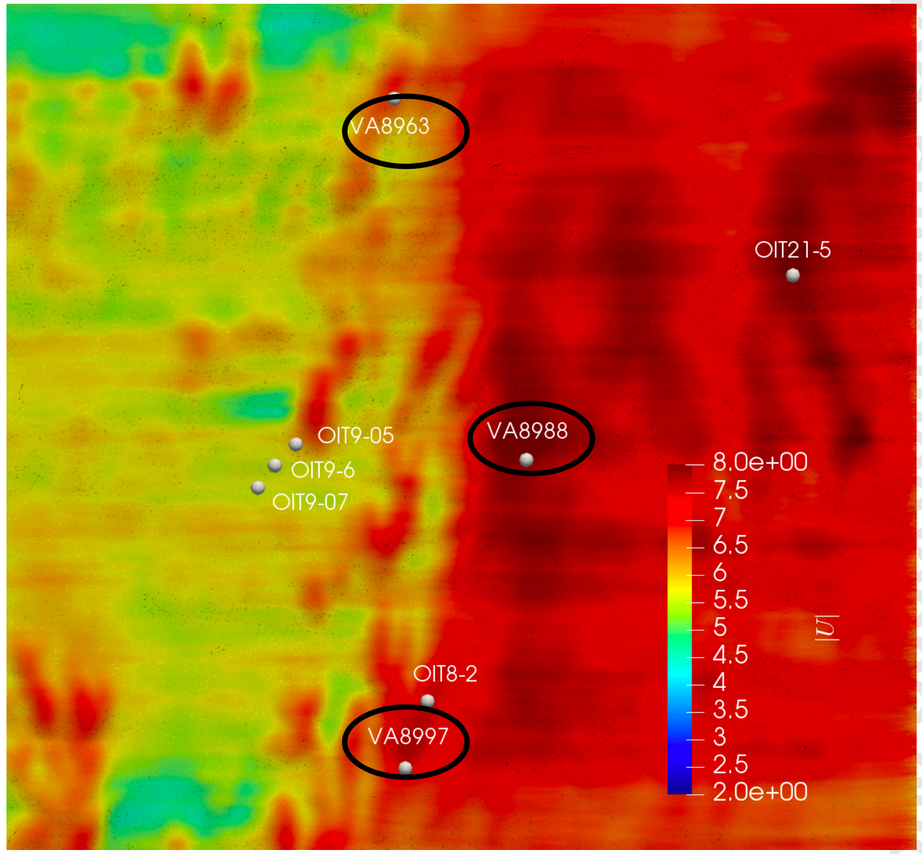
arcelona Supercomputing Center

IBERDROLA

Wind energy resource assessment



VA8963 VA8999 VA8997



arcelona Supercomputing Center

IBERDROLA

Conclusions

- A high-fidelity methodology for large scale simulation of turbulent flows by means of low dissipation FE has been presented.
- The methodology has been applied to carry out scale resolving simulation of industry relevant problems and validated with experimental data.
- Future work involves the extension to high order elements, compressible flows, the integration of non equilibrium wall models and mesh adaptability.

Thanks!

Barcelona Supercomputing Center